

## Review

## Radiation damage effects on zinc oxide (ZnO) based semiconductor devices – a review

Rosfayanti Rasmidi <sup>a,b</sup>, Mivolil Duinong <sup>a</sup>, Fuei Pien Chee <sup>a,\*</sup><sup>a</sup> Faculty of Science and Natural Resources, Universiti Malaysia Sabah, 88400, Kota Kinabalu, Sabah, Malaysia<sup>b</sup> Faculty of Applied Sciences, Universiti Teknologi MARA Sabah Branch, Kota Kinabalu Campus, Sabah, Malaysia

## ARTICLE INFO

## Keywords:

Zinc oxide  
Radiation damage  
Radiation tolerance  
Space application

## ABSTRACT

In space, semiconductor devices are vulnerable to various effect of high energy radiation, causing single event upsets (SEUs), damaging or altering the lattice structure of the semiconductor device. The effect of ionizing radiation on metal oxide semiconductor device had been receiving very little attention as most research focus on polycrystalline silicon-based semiconductor. Based on our previous research studies specifically on gamma radiation exposure, the interaction effects of radiation towards ZnO based semiconductors shows changes across all 4 different types of parameter, namely the morphology, structural and optical as well as the electrical properties. As a general classification, morphological change is attributed to the interaction within the crystal lattice, while structural distortion is due to high energy displacement cascade, whereas changes in the optical properties relates to the formation of colour centres (F-centre). The overall parametric changes will then affect the electrical properties as degradation of general parameters will lead to the increase of the ideality factor of the ZnO semiconductor device. The increase of the ideality factor after irradiation is attributed to the production of recombination centres in the space charge region. Furthermore, large values of the ideality factor, obtained after irradiation, point out extrinsic recombination mechanisms where the initial and final states of recombination are located at a lattice imperfection such as a dangling bond or a complex involving impurity atoms and vacancies. Therefore, in this paper a more thorough review of past research on the radiation related studies on ZnO is discussed. This review aims to provide an in-depth discussion on various radiation effects of zinc oxide based semiconductor devices.

## 1. Introduction

At present, the application of zinc oxide (ZnO) semiconductor from semiconductor group II-VI has become a prominent semiconductor material in fabrication as it possesses wide bandgap of 3.37 eV and high exciton binding energy of 60 MeV (Naz et al., 2018). Apart from that, ZnO also has a high electron mobility, easily fabricated under low temperature, efficient photon emission, can be easily n-doped, higher mobility than silicon-based thin film transistors (SiTFTs), low resistance, high transparency, high translucency (>80%) and high conductivity, low cost and non-toxicity (Morkoç and Özgür, 2009). Among metal oxide nanoparticles, ZnO has been the subject of focused research due to their extraordinary electronic, optical, mechanical, magnetic and chemical properties that are significantly different from those of bulk counterpart (Parihar et al., 2018). The advantages of ZnO could overcome the flaws substantially and replace the use of conventional SiTFTs

(You and Wang, 2017). A number of diverse methods had been used to fabricate ZnO channel layer including radio frequency (RF) sputtering (Hirao et al., 2007), metal organic chemical vapor deposition (MOCVD) (Remashan et al., 2012) and pulse laser deposition (PLD) (Luo et al., 2019).

Harsh environments present a severe challenge for designers of semiconductor devices and electronics whereby semiconductor systems must exhibit a high degree of radiation tolerance include electronics for use in space, critical systems for nuclear reactors, and detectors for particle beams and advanced light sources (Cressler and Mantooth, 2013). Radiation doses in such environments may present up to 40 Mrad, although in the most extreme conditions envisaged this value goes to 400–1000 Mrad depending on radiation type (Rahman et al., 2004).

Space application of oxide-based semiconductor material is starting to gain attention where its superiority over amorphous silicon-based material are greatly noticeable (Mishra and Adelung, 2018). When

\* Corresponding author.

E-mail address: [fpchee06@ums.edu.my](mailto:fpchee06@ums.edu.my) (F.P. Chee).

ZnO based films were irradiated with a total dose of 1.7 Mrads from  $^{60}\text{Co}$ , it shows degradation in the turn-on voltage and appearance of low frequency noise (Indluru et al., 2013) (L. Y. Liu et al., 2018). The electron mobility is found to benefit from the exposure and shows a significant increment. The changes in the electrical properties of the films are induced by the irradiation are attributed to the combination effects of interface states creation and electron-hole pair generation in the insulating layer (Indluru et al., 2013). The necessity of research on the durability of ZnO towards radiation exposure is vital as previous research reveals that the resistance of ZnO towards radiation effects was better than most conventional semiconductor materials and emerging transistor technologies (Ramirez et al., 2015).

In addition, the resistivity of indium-doped zinc oxide-based TFTs (IZO-TFTs) was discovered to increase significantly with increasing proton-irradiation doses up to  $10^{14} \text{ cm}^{-2}$  due to creation of point defects and structural amorphization. The field effect mobility and turn-on voltage of the IZO-TFTs decreases remarkably after the proton irradiation while the sub-threshold swing value shows a positive shift. These devices establish low sensitivities to post-thermal annealing due to the creation of antisite oxygen point defects (Ramirez et al., 2015). The IZO-TFTs, when irradiated with Cobalt-60 source, also shows degradation in the turn-on voltage and appearance of low frequency noise (Y. Liu et al., 2014) (Özgür et al., 2005). The electron mobility, however, is found to benefit from the exposure and shows a notable increment. The changes in the electrical properties of these IZO-TFTs induced by the irradiation are attributed to the combined effects of interface states creation and electron-hole pair generation in the insulating layer (Y. Liu et al., 2014).

In conventional covalent semiconductors, the chemical bonds are  $p$  or  $sp^3$  orbitals with strong directivity and radiation damage can lead to strained bonds and deep trap states.

In an amorphous state of these semiconductors, strained bonds and other defects lead to trap states, and the mobility of the amorphous semiconductors is much less than their crystalline counterparts. While for metal oxide based semiconductor such as ZnO, the cations in ZnO form states at the conduction band minimum from spherically extended  $s$  orbitals of the metals which in turn substantially reduces the role of disorder for conduction band transport because the orbital that overlaps with the adjacent spherical orbitals is largely unaffected by the disorder. (D. Zhao, 2010).

### 1.1. Overview of radiation study on metal oxide thin films

Extensive investigation of atomic displacement effects in solid did not begin until nuclear reactor development during World War II when Wigner suggested that neutrons produced as a result of nuclear fission would give an insight of systematically investigating displaced atoms in solids (Kinchin and Pease, 1955). The launching of artificial satellites in the late 1950s and the resulting discovery of the earth's radiation belts by Van Allen broadened the radiation environments of interest, to the radiation effects community, to include high energy electrons and protons. The radiation response of semiconductor devices, in particular, became a major area of study that included not only the effects of the natural environment but also those of nuclear weapons (Messenger and Ash, 1986). In contrast to the history of ionization effects, no single unit has emerged from displacement damage studies comparable to that used for absorbed ionizing dose. Instead, early studies tended to focus upon estimates of the number of displaced atoms produced in the target material as a first step in correlating a given property change with radiation exposure, usually measured as a particle fluence (Kinchin and Pease, 1955). Few attempts were made initially to correlate the damage produced by different radiations, and little success was achieved in using damage data obtained with one type of radiation to predict the effects produced by another. This was because it was widely believed that displacement damage produced by neutrons led to fundamentally different defect structures (large clusters) (Gossick, 1959) than to that

produced by electrons (point defects). Protons were generally assumed to generate a mixture of point defects and clusters. The view described above has changed in recent years because of several new experimental and theoretical results.

Based on research conducted by Nastasi et al. (1996), it was stated that bombardment of a crystal with energetic (kilo-electron volts to mega-electron-volts) heavy ion produces regions of lattice disorder. The disorder can be directly observed by techniques such as transmission electron microscopy, MeV-particle channelling, and electron diffraction. As an ion slows down and comes to rest in a crystal, it makes a significant number of collisions within the lattice atoms. In these collisions, sufficient energy may be transferred from the ion to displace an atom from its lattice site. Lattice atoms which are displaced by incident ion are called primary knock-on atoms (PKAs) (Nastasi et al., 1996). The PKAs can, in turn, displace other atoms, secondary knock on atoms, tertiary knock-ons and so on thus creating a cascade of atomic collisions (Amir and Chee, 2012) (Chee et al., 2019). This leads to a distribution of vacancies, interstitial atoms, and other types of lattice disorder in the region around the ion track. As the number of ions incident on the crystals increases, the individual's disordered regions begin to overlap. At some point, a heavily damaged layer is formed. The total amount of disorder and the distribution in depth depend on ion species, temperature, energy, total dose and channelling effects (Nastasi et al., 1996).

In a related study, the parameters that give effect to the formation of radiation damage are the ion mass, ion species, the target temperature during irradiation, total dose, ion's energy and the ion's flux (number of ions per unit area) (Pien et al., 2010) (Wesch et al., 2012). Studies of this ion-solid interaction can be done by introducing atoms into a solid substrate by the bombardment of the solid with ions in the electron-volt (eV) to mega electron volt (MeV) energy range. The physical properties for a certain solid substrate are sensitive to the presence of a trace number of foreign atoms. Mechanical, electrical, optical, magnetic and superconducting properties are all affected and sometimes may even be dominated by the existence of such foreign atoms (Chee et al., 2011).

Properties of metal oxides materials are directly or indirectly connected to the presence of defects, oxygen vacancies in particular (Kristianpoller et al., 2010). Point defects play a fundamental role in determining the physical and chemical properties of inorganic materials. This holds not only for bulk properties but also for the surface of oxides, where several kinds of point defects exist and exhibit rich and complex chemistry. Depending on the material electronic structure, the nature of oxygen vacancies changes dramatically. Examples include non-metal vacancy at metal/non-metal site, neutral vacancies, positively/negatively charged non-metal vacancies, free positive holes, etc. (E. Lee et al., 2010).

Oxygen vacancies are known as colour centres, or F centres (from Farbe, the German word for colour). It is believed that ionizing radiation causes structural defects, leading to a change in their density upon exposure to gamma-rays (Gupta and Gupta, 2016). Colour centres in oxide thin films, such as  $\text{WO}_3$  and  $\text{MoO}_3$ , had been observed by irradiation with UV light from a high-pressure lamp in the fundamental absorption region at a wavelength of 330 nm (Fortunato et al., 2005). The formation of colour centres has been associated with an increase in electrical conductivity, in which free electrons are produced as a result of band-to-band transitions and trapping of these electrons in oxygen ion vacancies (Haider and Chee, 2014). It was found that there is more than one type of defects responsible for the formation of colour centres in  $\text{MoO}_3$  thin films (Fortunato et al., 2005). Alternatively, both sputtered  $\text{SiO}_2$  thin films and fused  $\text{SiO}_2$  are identical in producing colour centres when they are bombarded by neutrons or X-rays (Burlacu et al., 2008). Arshak and Korostynska (2004) studied the effects of high-energy ions on the  $12\text{CaO}_7\text{Al}_2\text{O}_3$  films. Reportedly, the conductivity of the films was enhanced, and the films become coloured by irradiating with ultraviolet light due to the formation of  $\text{F}^+$ -like centres. The electrons forming the  $\text{F}^+$ -like centres are photo released from the encaged  $\text{H}^-$  ions, which are presumably derived from the pre-existing  $\text{OH}^-$  groups. The induced

electron concentration was proportional to the calculated displacements per atom, which suggests that nuclear collision effects of the implanted ions play a dominant role in forming the electron and H<sup>-</sup> ion in the films (Arshak and Korostynska, 2006). However, metal oxide involving the oxygen vacancies of ZnO thin films are yet to be discovered. It is generally accepted that two distinct processes are responsible for the formation of colour centres, following bombardment with ionizing radiation. The primary mechanism is in charge of defect formation, while the secondary one gives rise to the stabilization of the centres. The model for colour centre kinetics assumes that the level of the radiation damage should be dose rate dependent, because of the damage recovery (Lorenz et al., 2011). As colour centres are created under irradiation, they also annihilate even under room temperature. During irradiation, both annihilation and creation coexist. The colour centre density will reach equilibrium at a level, depending on the applied dose rate. The creation and annihilation constants can be determined by using experimental data obtained under one particular dose rate, and can then be used to predict the behaviour of the same sample under different dose rates (Lorenz et al., 2011). The overall response is roughly considered as three-staged, where the initial formation of colour centres (stage I) is followed by defects saturation (stage II), and concluded with a decrease in defect concentration (stage III). The primary process, which is active during all three stages, involves the non-radiative de-excitation of an exciton with the formation of a Frenkel pair (F centre and halogen interstitial) (Di et al., 2011). Pre-existing impurities and defects in the sensing material act as saturating traps, capable of stabilizing a limited number of interstitial atoms. The concentration growth occurring at stage I is due to the effective stabilization of the interstitial ions by the traps, initially present in the crystal. The saturation of the traps leaves the recombination of the interstitial atoms and F centres as the dominant process and leads to the flat region of stage II. During both stages, the contribution to the stabilization process due to the aggregation of the interstitial atoms is still negligible, although it becomes more significant, as the radiation dose increases. The interstitial aggregation finally dominates the stabilization mechanism when, during stage III, it allows a further increase in the defect concentration.

Pre-existing impurities and defects in the sensing material act as saturating traps are capable of stabilizing a limited number of interstitial atoms. According to that, the concentration growth occurring during stage I is due to the effective stabilization of the interstitial ions by the traps, initially present in the crystal. The saturation of the traps leaves the recombination of the interstitial atoms and F centres as the dominant process and leads to the flat region of stage II. During both stages, the contribution to the stabilization process due to the aggregation of the interstitial atoms is still negligible, although it becomes more significant, as the radiation dose increases.

In terms of metal oxides research, ZnO and Cu<sub>2</sub>O are considered to be one of the most notable materials due to its affordability and compatibility in a variety of electrical devices. In addition, it has riveting optical and I-V (current-voltage) properties. Research on p-type Cu<sub>2</sub>O and n-type ZnO based thin film heterojunction has received attention due to its deposition flexibility using various known methods such as magnetron sputtering (Ellmer et al., 2001), chemical vapor deposition (CVD) (Stavale et al., 2013), molecular beam epitaxy (MBE) (Liu Y et al. 2014) and electrochemical deposition (Ievskaya, 2014).

## 2. ZnO structure and chemical properties

Zinc oxide, with its unique physical and chemical properties, such as high chemical stability, high electrochemical coupling coefficient, a broad range of radiation absorption and high photostability, is a multifunctional material (Segets et al., 2009). In materials science, ZnO is classified as a semiconductor in group II-VI, whose covalence is on the boundary between ionic and covalent semiconductors. Wurtzite zinc oxide has a hexagonal structure (space group C<sub>6</sub>mc) with lattice parameters number  $a = 0.3296 \text{ nm}$  and  $c = 0.52065 \text{ nm}$ . The structure of

ZnO can be simply described as alternating planes composed of tetrahedral coordinated O<sup>2-</sup> and Zn<sup>2+</sup> ions, stacked *a* alternately along the *c*-axis (Fig. 1) (Wang, 2004).

A broad energy band (3.37 eV), high bond energy (60 MeV) and high thermal and mechanical stability at room temperature make it attractive for potential use in electronics, optoelectronics and laser technology (Bacaksiz et al., 2008) (Wang, 2004) (Venkatesh and Jeganathan, 2013). The piezo- and pyroelectric properties of ZnO indicate that it can be used as a sensor, converter, energy generator and photocatalyst in hydrogen production (Chaari and Matoussi, 2012). It can also be used in photo-electronic (Babamoradi et al., 2018) and electronic equipment (Locovei et al., 2019), in field emitters (Mishra and Adelung, 2018), in sensors (Kim et al., 2019), in UV lasers (Parikh et al., 2018). Because of its hardness, rigidity and piezoelectric constant, it is an important material in the ceramics industry, while its low toxicity, biocompatibility and biodegradability make it a material of interest for biomedicine and in pro-ecological systems (Özgür et al., 2005). Because of its diverse properties, both chemical and physical, ZnO is widely used in many areas. It plays an important role in a very wide range of applications, ranging from tyres to ceramics, from pharmaceuticals to agriculture, and from paints to chemicals.

One of the most important applications of ZnO in electronics is in the production of varistors (Gupta K.M. & Gupta N., 2016). These are resistors with a non-linear current-voltage characteristic, where current density increases rapidly when the electrical field reaches a particular defined value. They are used, among other things, as lightning protectors, to protect high-voltage lines, and in electrical equipment providing protection against atmospheric and network voltage surges. These applications require material of high compactness since only such a material can guarantee the stability and repeatability of the characteristics of elements made from it.

Space electronics, particularly thin film transistors (TFTs) on polymer substrates, are of growing importance for space exploration applications, such as solar sails, synthetic aperture radar systems, space-borne telescope and balloons (Indluru et al., 2013). Each of these applications requires distributed sensing and electronic health monitoring of thin, low mass and large area deployable structures which could not be implemented using conventional engineering materials such as metals and alloys (Zhou et al., 2004). However, operating environment of these devices during stowage and deployment is far from stable and not without interference, especially in outer space.

In recent years, space application of oxide based TFTs are started to receive some attention due to its superiority over amorphous-silicon TFTs. The resistivity of indium-doped zinc oxide-based TFTs (IZO-TFTs) was found to be increased dramatically with increasing proton-irradiation doses up to  $\sim 10^{14} \text{ cm}^{-2}$  due to the creation of point defects and structural amorphization. The field effect mobility and turn-on

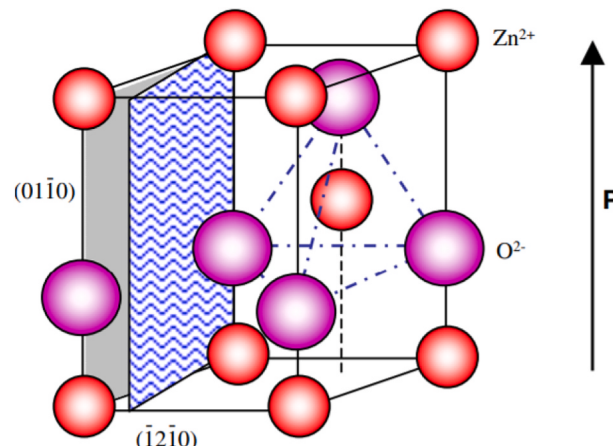


Fig. 1. The wurtzite structure model of ZnO (Wang, 2004).

voltage of the IZO-TFTs decrease noticeably after the proton irradiation while the sub-threshold swing value shows a positive shift. These devices establish low sensitivities to post-thermal annealing due to the creation of antisite oxygen point defects (Moon et al., 2010). The IZO-TFTs when irradiated with  $^{60}\text{CO}$  also shows degradation in the turn-on voltage and appearance of low frequency noise (Indluru et al., 2013) (Y. Liu et al., 2014). The electron mobility, however, is found to benefit from the exposure and shows a remarkably increment. The changes in the electrical properties of these IZO-TFTs induced by the irradiation are attributed to the combined effects of interface states creation and electron-hole pair generation in the insulating layer noise (Indluru et al., 2013).

### 3. Interaction of radiation with matter

When charged particles interact with matter, they lose energy to both ionizing and non-ionizing effects. The ionization is a process that strips electrons from atoms in the material, thereby creating ions. The electron excitation is the closely related mechanism of ionization. However, the excitation happens when the energy is less than the potential for ionization. The charged particle radiation such as alpha ( $\alpha$ ), beta ( $\beta$ ) and proton induce direct ionization to the material while neutral radiation such as neutron, and gamma ( $\gamma$ ) cause indirect ionization. The susceptibility of ionization damage varies with the type of bonding in the material. Metallic bonding holds positive ions together with free valence electrons. Ionization radiation excites the electron to higher energy level, but they relax to its original energy state shortly. Therefore, there is no permanent damage occurred due to the ionization of metallic bonding. Ionic bonding is weaker than metallic bonding in ionization prospect. In ionic bonding, one element transfers its loosely bound electron to another element to create positive ion (cation) and negative ion (anion). The electrostatic attraction and repulsion between cation and anion lead to a well ordered three-dimensional arrangement in the crystal structure. The ionization could create a higher positive charge in cation due to electron stripping and hence enhanced the attraction between cation and anion. However, the ionization effect is temporary in ionic bonding due to its fast recovery of the excited electrons. The covalent bonding found in compounds such as  $\text{H}_2\text{O}$ ,  $\text{CO}_2$ , Si,  $\text{SiO}_2$ , etc. shares outer electrons in a molecule between all the atoms. The resultant covalent molecules do not attract one another, and the energy of the bonding is in low eV range. Hence, the radiation has enough energy to separate the covalent molecule into its constituent atoms or radicals through ionization. Therefore, the original chemical composition of the material changes leaving permanent damage.

The atomic displacement primarily occurs through kinetic energy transfer or radiolytically by the conversion of radiation-induced excitation into atom motion (recoil). When a charged particle passes through the material, some of the particle's energy dissipates by exciting orbital electrons of the elements and by elastic collisions with the nuclei. The atomic displacement damage is a result of an elastic nuclear collision caused by the incoming energetic particle. Due to the elastic collision, the atom could eject from its normal lattice position. The ejected atom is known as a primary knock-on, which may cause a cascade of atomic displacements before coming to rest. The displaced atom becomes an interstitial, and its original vacant position in the lattice becomes a vacancy. Together the interstitial and the vacancy are known as a Frenkel pair. The displaced atom could continue the atomic displacement process with its excess transferred energy to create displacement cascade damage. The collisions are produced by both incident heavy particles such as protons, neutrons, ions and secondary particles (recoils). The defects are produced along the path of the displacement cascade. The atomic displacement damage initiates when the transferred kinetic energy via elastic collision surpasses the atomic displacement energy threshold of the particular element or the compound. Therefore, the atomic displacement energy threshold is one of a measure of radiation hardness of a material (Claeys and Simoen, 2002).

### 4. Details of radiation study on ZnO based semiconductor devices

#### 4.1. Proton damage on ZnO

In 2010, a research was conducted by Moon et al. (2010) on IZO-TFTs by exposing high-dose proton-beam irradiation on indium-doped ZnO based thin-film transistors (IZO-TFTs) to investigate the effect of irradiation on its performance by controlling their electrical and structural properties. The experimental specifications were prepared on  $\text{SiO}_2/\text{n-Si}$  substrates using DC magnetron sputtering. The target used in this study was a sintered ZnO-10 wt%  $\text{In}_2\text{O}_3$  ceramic target (99.999% purity, 100 mm dia.). Once the fabrication was completed, IZO-TFTs were irradiated by a high-energy 5 MeV beam at a dose of  $10^{10}$ – $10^{15}$  protons  $\text{cm}^{-2}$  to control the electrical properties in the ZnO channel layer (Moon et al., 2010).

The resistivity of IZO thin films dramatically increased with the increment of proton-irradiation doses up to  $\sim 10^{14}$   $\text{cm}^{-2}$ , after which the resistivity recovered to a level similar to as-deposited IZO thin film. After proton irradiation, the crystallinity of IZO thin films was reduced due to defect-isolation and/or chemical-isolation. The field effect mobility of IZO-TFTs decreased from  $2.20 \text{ cm}^2 \text{ V}^{-1} \text{ s}^{-1}$ – $1.22 \text{ cm}^2 \text{ V}^{-1} \text{ s}^{-1}$ , turn-on voltage shifted  $-7 \text{ V}$  to  $-21 \text{ V}$ , and subthreshold swing value increased after proton irradiation with a  $10^{12}$   $\text{cm}^{-2}$  dose. With proton-irradiation doses over  $10^{14}$   $\text{cm}^{-2}$ , IZO-TFTs device performance recovered to a level similar to that of a pristine device. Moreover, irradiated thin films and devices have low sensitivities to post-thermal annealing due to the creation of antisite oxygen point defects.

Based on the post irradiated x-ray diffraction results of the analysis, IZO thin films were strongly oriented in the (002) direction regardless of the increasing high-dose proton irradiation. When proton irradiation dose of  $10^{12}$   $\text{cm}^{-2}$  was applied to IZO thin films, the XRD peak intensity was lower than pristine films, and then further peak intensity was increased at proton-irradiation dose of  $10^{14}$   $\text{cm}^{-2}$ . An energetic proton penetrating through IZO thin films generates vacancies in both Zn and O sub-lattices and interstitials of different symmetries. These point defects created by proton irradiation play a role in the changing crystalline characteristics. From these results, it was concluded that proton irradiation slowly changed the structure of IZO thin films through amorphization (Moon et al., 2010).

The post result of the proton irradiation towards the effects on native point defects showed that with increasing dose of irradiation, the resistivity of IZO thin films increased gradually at relatively low proton-irradiation doses. Low irradiation dose associated with the creation of native point defects and damage-induced degradation of carrier mobility and crystallinity. In addition, it was observed that the atomic percentage of the related oxygen vacancies was decreased by high dose proton irradiation (Moon et al., 2010).

In another research conducted by Cheol Eui et al. (2010), a ZnO was hydrothermally grown with a thickness of 0.5 mm, of undoped n-type with (001) orientation. The prepared samples were then irradiated at room temperature by a 1.5 MeV proton beam at a dose of  $1 \times 10^{15}$   $\text{cm}^{-2}$ . Based on the Raman spectra irradiated and unirradiated ZnO, Raman shift of both states were recorded at a highest peak of  $436 \text{ cm}^{-1}$ . However, a prominent increase was recorded at the peak of  $576 \text{ cm}^{-1}$  for irradiated ZnO crystals. This can be attributed to existing defects within the crystals such as Zn vacancies, oxygen vacancies and Zn interstitials due to irradiation. Fig. 2 shows the Raman spectra of the ZnO single crystal before and after proton irradiation.

Referring to Fig. 2, a peak of about  $436 \text{ cm}^{-1}$  is assigned to the non-polar optical phonon ( $E_2$ ) modes of the virgin and the irradiated ZnO single crystal. The two non-polar low frequency  $E_2$  modes,  $E_2$  (low), and the high frequency,  $E_2$  (high), are Raman active only. The sharpest and strongest peak about  $436 \text{ cm}^{-1}$  can be assigned to the high-frequency branch of the  $E_2$  mode  $E_2$  (high) of ZnO, which is the strongest mode in the wurtzite crystal structure. A strong  $E_2$  (high) mode indicates good

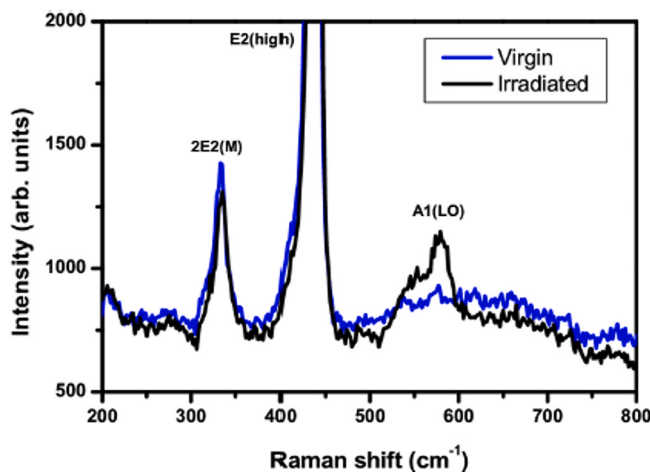


**Fig. 2.** Raman Spectra of the ZnO single crystal before (Virgin) and after proton irradiation (Cheol Eui et al., 2010).

crystallinity, and the  $E_2$  (low) mode of ZnO is associated with the vibration of the heavy Zn sublattice.

An intense peak at  $436\text{ cm}^{-1}$   $E_2$  (high) and  $330\text{ cm}^{-1}$   $2E_2(M)$  is known to be the vibration mode associated with multiple-phonon scattering processes. In addition, a weak peak is seen at  $A_1(LO)$  mode at  $576\text{ cm}^{-1}$  in the Raman spectrum of the as grown ZnO single crystal has been reported to be enhanced by disorder induced by ion bombardment where the polar  $A_1(LO)$  mode can split into transverse optical and longitudinal optical phonons, both being active in Raman and infrared spectroscopy. A prominent increase however is seen at  $A_1(LO)$  mode at  $576\text{ cm}^{-1}$  which is attributed to proton irradiation. The increase is due to a large number of defects, such as Zn vacancies ( $V_{\text{Zn}}$ ), O vacancies ( $V_{\text{O}}$ ), and Zn interstitials ( $\text{ZnI}$ ), generated by the irradiation (Shi et al., 2002) and can break down wave vector conservation in the Raman scattering process, making scattering events from the whole Brillouin zone possible and disorder-activated Raman scattering visible.

Based on the PL spectra results, a sharp UV emission spectra at  $380\text{ nm}$  was seen for irradiated ZnO crystals which were attributed to the free exciton recombination at room temperature due to large exciton binding energy of ZnO ( $60\text{ MeV}$ ) (Cheol Eui et al., 2010). The most obvious change after proton irradiation was linewidth broadening of the green emission and a strong decrease in the PL intensity. If the radiation-induced change in the luminescence spectra had to do with damage in the oxygen sublattice, oxygen vacancies should be involved in the  $550\text{ nm}$  band quenching (Cheol Eui et al., 2010). It appears then that oxygen vacancies can have contrasting effects on the green luminescence in different experiments. A high concentration of radiation-generated oxygen vacancies has a quenching effect while the vacancy concentration, produced in a reducing thermal treatment, favours the green emission. The present work showed a complex influence of defects in the oxygen sublattice on the PL spectra, not excluding the influence of zinc vacancies (Cheol Eui et al., 2010). Fig. 3 shows the PL emission spectra of a single crystal of ZnO prior to and after proton bombardment.

On the cathodoluminescence (CL) spectra of the ZnO crystal, a more apparent result can be seen in the green band excitation. The oxygen defects are known to give rise to the green emission and the width of the electron depletion region, where a width dictates a weaker green emission intensity for a given penetration depth of the electron beam. Fig. 4 shows the CL spectra of the ZnO crystal surfaces before and after proton irradiation.

The main difference between that of a PL and CL is the emission of light when stimulated by a light source, whereas a photon generates only one electron-hole pair, one 20 keV electron, for example, can generate thousands of electron-hole pairs in the extinction volume, which is

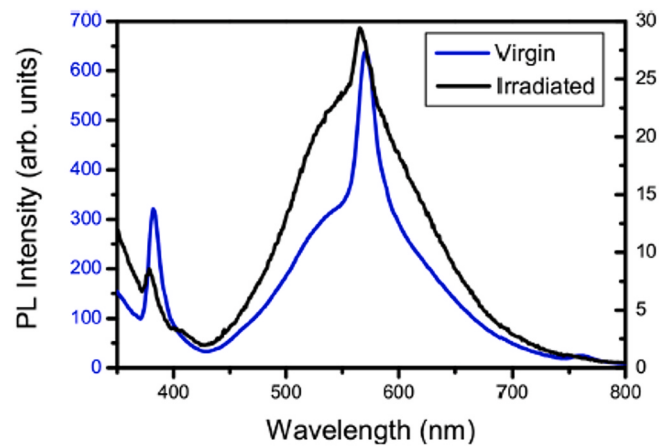


**Fig. 3.** PL emission spectra of the ZnO single crystal before (Virgin) and after proton irradiation (Cheol Eui et al., 2010).

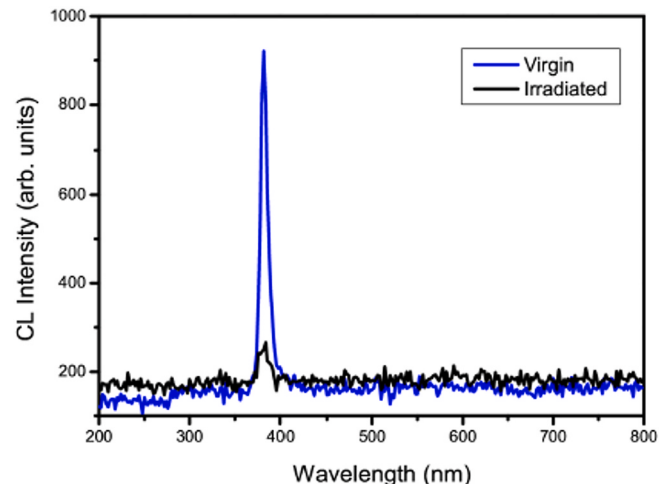


**Fig. 4.** CL spectra of the ZnO crystals surfaces before (Virgin) and after proton irradiation (Cheol Eui et al., 2010).

usually several microns in diameter. This is also important to emphasize the difference in the excitation volumes of a thin target or a bulk sample. At  $300\text{ K}$ , the intensity of the UV emission peak decreases with increasing proton irradiation. Since high-energy irradiation produces defects on the zinc sublattice, which can trap electrons, the oxygen vacancies are observed in crystals irradiated above the zinc displacement threshold energy in the form of Farbe + centres (Colour centre) instead of the neutral Farbe centres that are normally present. The spectral changes observed in the surface regions of the irradiated samples are surface effects not related to the radiation-induced point defects that extend deeper into the crystal.

In 2017, the effects of low energy proton beam irradiation on structural and electrical properties of ZnO:Al thin films were studied by Sahoo et al., (2017). The samples were deposited onto a silicon substrate using three targets DC magnetron sputtering system with a base pressure of  $8 \times 10^{-6}\text{ mbar}$  and working pressure of  $1 \times 10^{-3}\text{ mbar}$  under the ambience of pure Ar atmosphere, a power of  $400\text{ W}$ . The deposition was carried out to obtain a thickness of  $144 \pm 5\text{ nm}$ . The fabricated samples were then furthered annealed at  $600\text{ }^{\circ}\text{C}$ . Prepared samples were then irradiated with a proton beam at four different fluences ( $1 \times 10^{12}$ ,  $3 \times 10^{12}$ ,  $1 \times 10^{14}$  and  $3 \times 10^{14}\text{ ion/cm}^2$ ) with an energy  $100\text{ keV}$ . Prior to the physical irradiation process, the longitudinal straggling and lateral straggling were calculated using Stopping Range in Ion Matter (SRIM)-2008. The simulation results showed a value of  $118.8\text{ nm}$  of

longitudinal straggling and 138.4 of lateral straggling. Based on the obtained result referring to the Williamson plots, the electronic energy loss of 172 eV/nm dominates over the nuclear energy loss of 0.379 eV/nm. The domination nature of electronic energy loss may ionize a target atom or excite the electrons of the target atoms to a conduction band or give plasmonic effect. The estimated penetration depth of the proton energy of 100 keV irradiated on ZnO thin film is 628.0 nm. As the deposited thin film is within the threshold limit of the penetration depth, implantation is successfully avoided. Based on the XRD result obtained, the normalized peak (002) shows the peak shifting towards higher 2 theta angles with increasing irradiations fluences, indicating the existence of stress in the films. By using Scherer's equation, the full width half maximum (FWHM) of the samples were decreased with increasing grain size. Based on the reported data, the changes in the FWHM was proportional to the effects of annealing. The fabricated samples of ZnO: Al is 0.70° with a 9.04 nm crystallite grain size, while annealed sample at 600 °C shows an FWHM of 0.59° with a 11.03 nm. Samples irradiated with four difference fluences shows that with increasing dose, the FWHM expands up to 0.65° at maximum fluence which suggests the degradation of the crystallite grain size. The crystallite ordering increases for the films irradiated with higher fluences. There is no significant change in carrier concentration after irradiation, but the mobility and resistivity changes with the change in fluences. The mobility of the fabricated paired with annealing samples were 1.09 cm<sup>2</sup>/V with a resistivity of  $6.3829 \times 10^{-3}$  Ω/cm. At mid-range of proton fluence, the changes were observed to be 2.98 cm<sup>2</sup>/V with a resistivity of  $3.642 \times 10^{-3}$  Ω/cm. The homogeneity distribution of particles increases with the increase in fluence of the irradiation. The increase in activation energy of particles by low energy proton irradiations at higher fluences in the annealed Al-doped ZnO thin films were observed. In subsequent research, Sahoo et al. (2018) conducted similar studies, however, findings suggest a similar trend to that of 2017.

#### 4.2. Electron damage on ZnO

In another research conducted by Xie et al. (2006), it was reported that the enhanced UV emission of various kinds of ZnO by electron irradiation is attributed to the improvement of electron stimulated desorption of adsorbed water in the film. Based on their findings, under electron-beam irradiation on various kinds of ZnO samples prepared using a wet chemical method, it was observed that electron-beam irradiation could significantly enhance the UV emission of all the ZnO samples while reducing their visible emission. Prior to irradiation exposure, ZnO sample exhibited a UV emission at ~385 nm due to near-band-edge recombination. However, after electron-beam irradiation for 60 s, all the samples showed a significant increase in UV emission intensity, despite their morphologies, structures, and defect/impurity concentrations. The enhanced UV emission is due to the recombination based defect reaction facilitated by the oxidic layer. Based on earlier reports, the effects of electron beam irradiation towards ZnO capped with AlO<sub>x</sub> was strongly enhanced by electron beam irradiation (Hui et al., 2005), which corresponds to the research conducted by Xie et al. (2006). Both of the research (Hui et al., 2005; Xie et al., 2006) shows similar trend to the effects of electron bombardment on the material properties of ZnO thin films that electron bombardment could be associated with thermal annealing treatment.

Karuppasamy and Subrahmanyam (2007) conducted research specifically on the effects of electron bombardment on the properties of ZnO thin films. The ZnO thin films were deposited on to a quartz and glass substrates by electron beam evaporation with ZnO pellets with a purity of 99.9%. The samples were irradiated under a vacuum of  $5 \times 10^{-5}$  mbar, with an electron beam density of 10<sup>6</sup> W/cm<sup>2</sup> for 3 s. Based on their research findings, the irradiated samples were found to be in crystalline properties while the un-irradiated samples had an amorphous structure based on the broad wave diagram obtained from the x-ray diffractometer (XRD). Based on the data obtained from the XRD result, the

calculated grain size obtained showed a larger grain size in comparison to the unirradiated samples. On the optical properties, a decrease in the transmittance can be observed from the irradiated ZnO films. The decrease in its transmittance can be attributed to the loss scattering by the surface crystallites as well as the surface roughness due to soft cracks developed in the thin film. However, the decrease in the transmittance was close to the wavelength of 380 nm, which correspond to the fundamental absorption edge of ZnO thin films. Based on the transmittance data obtained, the calculated band edge showed a decrease from 3.28 eV to 3.26 eV. This leads to the understanding that a redshift in the bandgap has occurred. The possibilities on the redshift can be attributed to the presence of oxygen vacancies or due to electron bombardment. However, it was justified that there was no electron beam induced defects. In comparison to a sample that was thermally annealed at 800 °C, it was reported that the heating effect of electron bombardment is found to be distinct and different from conventional thermal annealing, where ZnO thin films that were annealed shows an improvement on its transmittance from 76% to 80% and increase in its bandgap contrary to that of the electron irradiated samples.

In 2009, Gür et al. studied the radiation hardness of ZnO thin films. The preparation of the samples was grown under different oxygen flow rates by electrochemical deposition onto commercial indium tin oxide substrates. XRD measurements showed that films are highly (002) c-axis oriented. It has been observed that the growth rates of the films are highly dependent on the oxygen flow rates. The high growth rate was obtained for the mid oxygen flow rates in the cell. Calculated crystallite size values had an increasing trend as the oxygen flow rate increases. Absorption measurements have revealed that the bandgap energy of ZnO thin films was about 3.4 eV. PL measurements showed that three emissions are observed in all films: free exciton emission at about 3.14 eV, 3.37 eV and so-called blue emission at 2.66 eV in ZnO. Relatively low dose  $5 \times 10^{12}$  e<sup>-</sup>/cm<sup>2</sup> and high-energy electron-irradiation (HEEI) 12 MeV experiments were performed on all films. The irradiation was performed at room temperature at a current density of around 0.3 A/cm<sup>2</sup>. Photoluminescence measurements result in three emissions in all films: UV 365 nm, UV1 395 nm, and blue 466 nm emissions in ZnO. After high-energy electron irradiation, a new PL emission, so-called green emission 520 nm, appeared, and the origin of the green emission is explained as the oxygen vacancy. One can deduce that the normalized intensity of the green emission decreases as the oxygen pressures increase inside the growth cell. The result shows that the impact of the high-energy electron irradiation is very low for the samples grown at high oxygen pressures. The annealing process gives rise to the recovery of the high energy electron-induced defect states, namely, V<sub>o</sub>.

Based on research conducted by Klochko et al. (2019), the effects of high doses of electron beam on ZnO was discussed. The ZnO films on flexible substrates, namely ZnO/PI and ZnO/PET, were deposited through SILAR method using adhesion seed layer and sulphate cationic precursor. Furthermore, the influence of high doses of electron beam irradiation towards uncoated PET, PI, glass and FTO substrates were investigated. The samples were irradiated with an electron irradiator on the base of transmission electron microscope (TEM) of EMV-100 BR brand. The electron beam accelerating voltage in all experiments was kept constant 75 kV, so the electron beam energy was 75 keV with irradiation time ( $\tau$ ) in the range from 20 to 3600 s and e-beam-doses current densities from 0.08 to 6.65 A/m<sup>2</sup>, which correspond to high e-radiation absorbed doses in the range of  $1.36 \times 10^8$ – $2.91 \times 10^{11}$  Gy, and too big total fluence from  $6.37 \times 10^{15}$  to  $1.50 \times 10^{19}$  e<sup>-</sup>/cm<sup>2</sup>. Based on the research findings, the influence of electron beam irradiation in vacuum, which doses exceed the conditions of long-term space applications are manifested in the form of ZnO defect in the slight electron-induced degradation of their structure, which is partially offset associated to thermal annealing. At the same time, such high absorbed doses of electron irradiation adversely affect all kinds of substrates. Thus, polymeric polyimide and polyethylene terephthalate flexible substrates at high absorbed doses of e-irradiation were not only

darkened but also cracked, attributed to the heat presence due to electron beams. On the substrate condition, post-electron irradiation shows degradation on the soda-lime glass substrates with a dark brown spot visible to the naked eye and SEM analysis on the crystallized channels. For FTO substrates, similar to that of polyethylene terephthalate, a darkened glass was reported and was very heavily etched at high absorbed doses of electron beam irradiation in comparison to pre-irradiated samples.

#### 4.3. Effect of gamma irradiation on zinc oxide based semiconductor

Over the years, research interest on ZnO based semiconductors has risen due to its superiority towards conventional based silicon-based semiconductors for space application. Based on a study conducted in 2010 (D. Zhao et al., 2010), ZnO TFTs were fabricated on borosilicate glass and polyimide substrate. The specifications were 54 nm thick Al<sub>2</sub>O<sub>3</sub> and 10 nm undoped ZnO, deposited at 200 °C by plasma enhanced atomic layer deposition (PEALD) and were then passivated 30 nm atomic layer deposition (ALD) Al<sub>2</sub>O<sub>3</sub>. The fabricated device was then exposed to a Cobalt-60 gamma rays (<sup>60</sup>Co) source with dose ranging 10 kGy to 1 MGy. The corresponding results show that irradiated devices have a negative threshold voltage of ~1 V for 10 kGy dose, increasing to ~1.5 V for 50 kGy and continues to increase with dose. The mobility of the irradiated device is nearly unchanged. The saturation of threshold voltage shift indicated self-annealing at the irradiation temperature (35–40 °C). On the recovery of the device, both the threshold voltage and turn-on shifts are entirely removed by annealing at 200 °C for 1 min. Also, the recovery of the device can be seen even at room temperature. The circuits operated well even after post-irradiation, with an increase in turn-on-voltage and increased oscillation frequency. Irradiation results for both devices and circuits on polymide substrates are similar to those found on glass substrates. These results show that PEALD ZnO TFTs and circuits are notable candidates for harsh radiation environments.

Ramirez et al. (2015) proposed two similar studies with dose ranging from 250 kGy to 1 MGy. A ZnO TFTs was fabricated on a borosilicate glass substrate. The thickness, however differs where the thickness of the gate dielectric used was 32 nm thick Al<sub>2</sub>O<sub>3</sub>. The deposition technique used was the same as previous research conducted by Zhao et al. (2010) using PEALD with a deposition temperature of 200 °C. The data obtained from both studies conducted by Ramirez et al. (2013) suggests that despite the difference in the ionizing dose, both devices under irradiation with electrical bias, results from incrementing of current sub threshold during irradiation, but immediately returns to its pre-irradiation value when removed from the gamma ray flux, suggesting a measurement artifact during irradiation. It is also apparent that most of the changes occurring in the ZnO devices occur for high dose as degradation of the ZnO performance is affected with increased dose. In this work, the irradiated devices are measured in air. Because of the gamma ray flux, the air surrounding the TFTs is partially ionized when the TFT is in its OFF stage (<1 V), the negative gate voltage will attract positive ionized charge at the back surface. This charge will shift the device characteristics negative and will be seen as an apparent increase in subthreshold current, which is in good agreement to the research conducted by Zhao et al. (2010). The charge is only partially bound, and even a positive gate voltage is sufficient to remove much of the charge. The first sweep with irradiation shows a small increase in subthreshold current, but current is greatly reduced for subsequent (voltage gate to source) V<sub>GS</sub> sweeps throughout the gamma ray exposure. The devices show virtually no shift in (voltage threshold) V<sub>TH</sub> during or after exposure for a cumulative dose of 240 krad. These results show that the statement from Zhao et al. (2010) on ZnO TFTs resistance against harsh radiation environments is valid. Referring to Table 1, radiation effects towards the structural properties of ZnO films shows degradation in both the grain size and strain. This indicates that while ZnO is naturally radiation resistant (Chee et al., 2019), the effects of

**Table 1**

Values of grain size and strain of un-irradiated and irradiated ZnO films (D. Zhao et al., 2010).

Zinc Oxide	Grain size (nm)	Strain
Un-irradiated	1108	0.48
Irradiated	880	0.33

radiation degrades the structural properties of ZnO. Fig. 5 shows the comparison made between other semiconductor devices. It can be observed that ZnO TFTs show relatively small changes with large radiation dose as compared to silicon and single wall carbon nano tube.

In 2014, Badawy et al. (2014) conducted a study on the structural and electrical impact of ZnO based semiconductors due to gamma-ray and calcination temperature. ZnO/TiO<sub>2</sub> powders were synthesized by utilizing the sol-gel method using ammonium hydroxide. The effects of calcination temperature (500–1000 °C) and gamma rays (with doses from 25 to 150 kGy) on the phases present and their electrical properties were investigated. The results revealed that heating the system at 500 °C led to the formation of ZnTiO<sub>3</sub>-rohom and TiO<sub>2</sub>-rutile. The degree of crystallinity of the phases produced increased by increasing the calcination temperature. When heating at 1000 °C, ZnTiO<sub>3</sub>-rohom turned to ZnTiO<sub>3</sub>-cubic but the rutile phase remained stable. Gamma irradiation causes the crystallite size of the rutile phase considerably from 146 to 63 nm and that of ZnTiO<sub>3</sub>-cubic decreased from 101 to 39 nm. This treatment also led to the creation of holes in the matrix of irradiated solids which increased the mobility of charge carriers (electrons) leading to a significant increase in the electrical conductivity reaching to 10<sup>2</sup> to 10<sup>3</sup>-fold. The produced holes facilitate diffusion of carriers across the matrices of the irradiated solids resulting in an effective increase in the electrical conductivity subsequent decrease in the activation energy.

Salari et al. (2018), conducted a research on the electrical characteristic of ZnO diode with an Au–Sb(n-Si ohmic contact), a Zn contact and ZnO as its active layer onto a Si wafer piece of (100) orientation. The samples were then subjected to gamma-radiation. Based on the semi log of the I-V characteristic, the leakage current has been increased with radiation exposure which corresponds to the decrement of the barrier height and an increase in its ideality factor of the diode. Due to the exposure of gamma radiation, the defects can be created within the crystal lattice structure. The drop of its barrier height as calculated were 0.774 eV (un-irradiated) and 0.742 eV (irradiated) respectively, while

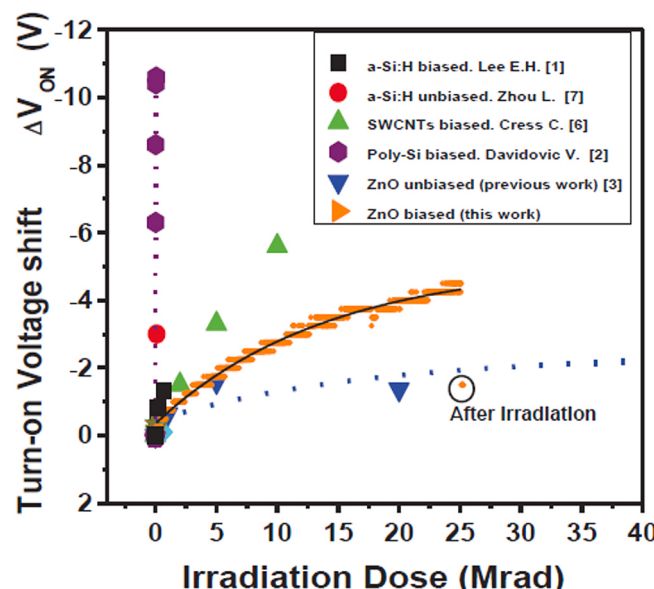


**Fig. 5.** Comparison of turn-on voltage shift as a function of irradiation dose for different material systems (D. Zhao et al., 2010).

the drop on its ideality factor is calculated to be 2.15 (un-irradiated) and 2.45 (irradiated). It was deduced that the electrical characteristic of proposed structure is sensitive to gamma radiation as the increase of its ideality factor suggests that its ideal state as a diode is decreased, in addition to its decrement on its barrier height. The degradation may be due to the radiation induced interfacial defects and lattice defects due to displacement damage. The increase on the leakage current with dose, on the other hand, is due to the generation carriers in the depletion region attributed to gamma irradiation which in turn induce lattice defects as the reverse leakage current is directly proportional to the concentration of the minority carriers that exist at junction. Based on the increase of the leakage current, a conclusion was raised which suggests that the existence of post-irradiated defects might very well be due to the generation recombination, interfacial oxide layer, tunneling and interface impurities as the possible factors attributing to the degradation of the diode.

Based on a study that was made by K. K. Lee et al. (2018), research was done on the reliability of gamma irradiated n-channel ZnO thin film transistors. The sample was prepared onto a borosilicate glass as the substrate. The prepared samples were then irradiated in incremental doses up to a total dose of 60 kGy ( $\text{SiO}_2$ ) with a  $^{60}\text{Co}$  source at 2.44 Gy ( $\text{SiO}_2$ )/s and at  $298 \pm 0.1$  K. The irradiation was performed while keeping the source and drain terminals grounded, and the gate dielectric field at +0.5 MV. Prior to irradiation, the transistors demonstrate good enhancement mode characteristic with excellent gate controlled of the linear and saturation operation regimes. The devices were irradiated with gamma-rays to total doses spanning from 1 to  $\sim 60$  kGy ( $\text{SiO}_2$ ). The degradation in mobility is correlated with the build-up of interface traps. An empirical equation relating the mobility to the radiation-generated interface trap density was found to provide a good fit to the experimental data. This expression could be used to predict the performance of irradiated devices. The threshold voltage is seen to increase by 2.5 V for the first 40 kGy ( $\text{SiO}_2$ ), then decrease slowly with further irradiation dose. This shift in the threshold voltage should not significantly affect the addressing of AMFPI pixels since the TFTs act as switching elements. Moreover, in most medical applications, the accumulated dosage is usually lesser than 10 kGy ( $\text{SiO}_2$ ). In the case of more complex circuits, the shift can be corrected through gain and offset corrections routinely employed in post-processing of image frames. In addition, the density of grain-boundary traps was not found to be affected by the irradiation. Possible reasons were provided by the enhanced radiation tolerance of grain-boundaries of ZnO. The results of this study are encouraging and demonstrate that ZnO-based TFTs fabricated via low-temperature processing can be used in applications involving high level of dose.

In a separate study conducted by Tashiro et al. (2019), the effects of gamma ray irradiation on the resistivity In ZnO bulk single crystals. A (001) oriented ZnO bulk single crystals with a thickness of 500  $\mu\text{m}$  were used in this study. The crystals were irradiated under a cobalt-60 source with an energy of 1.17 and 1.33 MeV with a total ionizing dose of 170 kGy. Based on the data obtained, the resistivity of the ZnO decreases from  $4.1 \times 10^4 \Omega \text{ cm}$  (at room temperature) to  $3.1 \times 10^2 \Omega \text{ cm}$  (irradiated). After the irradiation, slight increase in green luminescence at around 530 nm is observed, suggesting that zinc vacancy, oxygen vacancy and oxygen interstitials are induced by Compton electrons emitted by the gamma-ray irradiation because this photoluminescence peak is a superposition consisting of the emissions relating to the zinc vacancy of ( $\sim 490$  nm), oxygen vacancy ( $\sim 530$  nm), and oxygen interstitial of ( $\sim 580$  nm). The PL intensity of oxygen vacancy is eight times larger than that of zinc vacancy. The existence of oxygen vacancy ( $g$  value is 1.996) is also observed by the electron paramagnetic resonance. This signal disappears by illuminating red LED with a wavelength of 654 nm, indicating oxygen vacancies + to defect localized state + transition. The existence of zinc vacancy would suggest the formation of zinc interstitial (Zni). In analogy with the low resistivity after Al-implanted ZnO, the origin of the low resistivity in gamma-ray irradiated ZnO is attributed to the Zni located at  $\sim 30$  MeV below the conduction band.

On the optical characteristic, it was reported that the exposure of gamma-irradiation causes a shift on the transmission edge towards a greater wavelength indicating a decrease in the optical energy gap value due to the increase in the energy width of the band tails of localized states which agrees to the previous known research (A. Al-Hamdan et al., 2014) (Al-sofany et al., 2014). It is also reported that the band gap is decreased and absorption coefficient ( $\alpha$ ) is increased after irradiation. This indicates that the exposure of gamma ray irradiation affects the optical constants and the dispersion parameters of the ZnO thin films.

In a related study, Al-sofany et al., 2014 conducted a study on the effect of gamma ray exposure on aluminum doped with ZnO that was prepared using the same method using DC-magnetron sputtering. Based on the data that was obtained, it was stated that the optical band gap decreases after irradiation. The effects of the irradiation also lead to the formation of localized states due to structural defects on the thin film structure which leads to a decrease in the transition probabilities into the extended state, which results to the decline of the optical energy band gap which agrees to the previous research conducted by A. Al-Hamdan, D. Al-Alawy, and J. Hassan (2014).

On the refractive index of the thin film properties, it is reported that exposure of gamma irradiation causes its value to increase whereby previous studies suggested that it is attributed to the formation of crystal defects caused by the irradiation (A. Al-Hamdan et al., 2014) (Al-sofany et al., 2014).

#### 4.4. Neutron damage on ZnO

Based on a research conducted by Lorenz et al. (2011), a study was made on the radiation impact of neutron towards ZnO. For the preparation of ZnO ( $\sim 3 \mu\text{m}$  thick) layers, the use of a metal organic chemical vapor deposition (MOCVD) onto a (0001) sapphire substrate, were used for the neutron irradiation studies. The prepared samples were then irradiated in the 1 MW Portuguese Research Reactor (RPI) with a thermal neutron fluence with a rate of  $2.8 \times 10^{13} \text{ n/cm}^2/\text{s}$  (E1 MeV), an epithermal fluence rate of  $0.1 \times 10^{13} \text{ n/cm}^2/\text{s}$  (at 1 eV) and a gamma dose rate of  $2 \times 10^6 \text{ Gy/h}$ . For the irradiation process, samples were shielded inside Cd boxes, in order to reduce the thermal neutron component while others were irradiated with the full spectrum. ZnO was irradiated for 240 h and shielded inside Cd boxes (240f). The fast neutron fluences reached after 240 h and 480 h were  $0.5 \times 10^{19} \text{ n/cm}^2$  and  $1.0 \times 10^{19} \text{ n/cm}^2$ , respectively. The temperature during the irradiations was less than 70 °C. The fabricated ZnO sample was annealed for 20 min at 800 °C in air.

Based on their findings, ZnO shows a different behaviour upon neutron irradiation. Based on the structural analysis, the lattice parameters after irradiation changes moderately with ( $a = 3.252 \text{ \AA}$ ,  $c = 5.204 \text{ \AA}$  in the as-grown and  $a = 3.251 \text{ \AA}$ ,  $c = 5.206 \text{ \AA}$  in the irradiated sample). Furthermore, the XRD analysis shows a drop in the intensity in the irradiated samples and even more in the irradiated and annealed samples. A strong degradation is reported with the grown samples having a homogeneous surface and becomes inhomogeneous over wide regions after neutron irradiation with blistering and exfoliation more apparent for irradiated samples as shown in Fig. 6.

On the PL spectra of ZnO, the irradiation causes a strong decrease of the intensity near the band gap emission and introduced a strong defect related emission band in the red spectra region ranging around 1.8 eV. However, thermal annealing treatment shows partial recovery and the defect band shifts to higher energy (around 2 eV). The PL spectra is as shown in Fig. 7.

In the closest year, research conducted by X. Zhao et al. (2019) reported on the effects of neutron irradiation effects towards ZnO nanostructure. The samples were prepared through the use of a chemical vapor deposition (CVD) through a Zn powder reacting with oxygen under a deposition temperature of 800 °C for 30 min. The prepared samples were then irradiated with a fluence of  $10^{15} \text{ n/cm}^2$  at the Northwest Institute of Nuclear Technology. From the results obtained, it

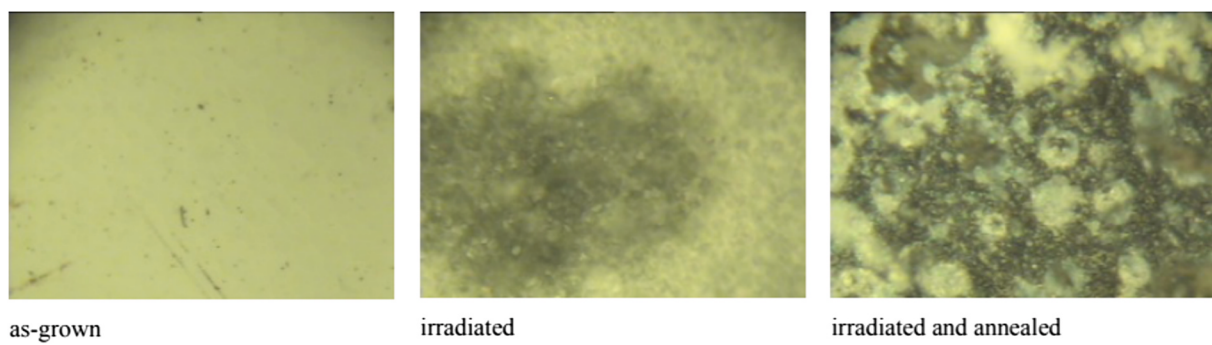


Fig. 6. Optical microscope images ( $300 \times 400\mu\text{m}$ ) of the as grown, irradiated, and irradiated and annealed ZnO samples (D. Zhao et al., 2010).

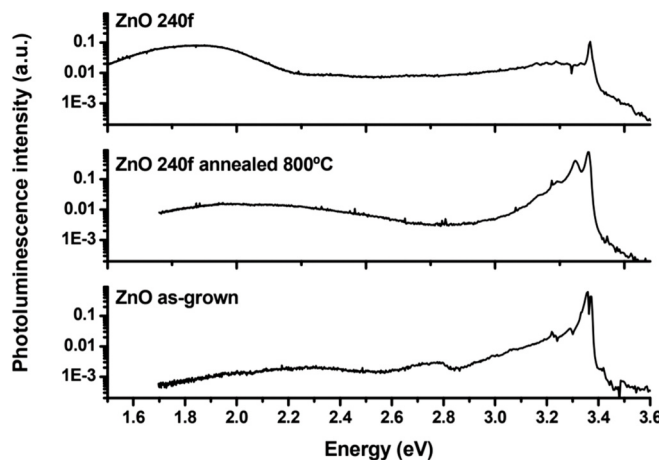


Fig. 7. PL spectra of as-grown and neutron irradiated ZnO before and after annealing at  $800^\circ\text{C}$  (D. Zhao et al., 2010).

was reported that the ZnO nanowires maintain their basic structures with a significant change observed in their diameter which is attributed to the neutron bombardment which causes the nanowire to break. Fig. 8 shows the SEM images of the grown samples and irradiated ZnO nanowires.

Based on the PL spectra of the ZnO nanowire samples, a small red shift can be observed for the irradiated samples which suggest that the irradiated ZnO nanowires experience a minor defect generated (X. Zhao et al., 2019). The PL spectra between irradiated and unirradiated samples are as shown in Fig. 9.

In separate conduct, irradiated ZnO nanoflakes cause atoms to break away from the surface resulting in large vacancies in the ZnO as shown in Fig. 10.

Based on the PL spectra, a shift of  $3.10\text{ eV}-3.13\text{ eV}$  indicating a blue shift due to the formation of ZnO nanoparticles. The PL spectra of the nanoflake are as shown in Fig. 11.

The neutron-irradiation effects of CVT grown ZnO nanowires and nanoflakes were investigated in this paper. The ZnO nanowire structure is more stable than the nanoflake structure for the neutron irradiation. After the  $10^{15}\text{ n/cm}^2$  neutron irradiation, the nanowires' diameters were decreased and the nanoflakes were transformed into nanoparticles. The near band emission (NBE) red shift of the irradiated ZnO nanowires indicates the shallow defects generated. The NBE blue shift of the ZnO nanoflakes is consistent with the transformation of nanostructure. The structure deformation induced by neutron irradiation can be used in the preparation of different nanostructures.

Based on the reported data, the neutron irradiation effect towards CVT deposited ZnO nanowires and nanoflakes indicate that ZnO nanowires show higher stability in comparison to ZnO nanoflake structure under a fluence of  $10^{15}\text{ n/cm}^2$ . On the structural changes, the nanowires

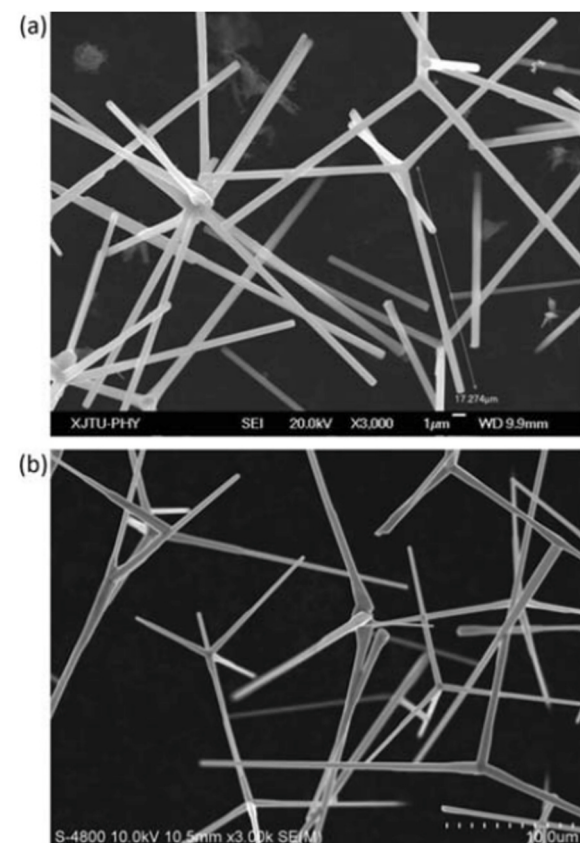
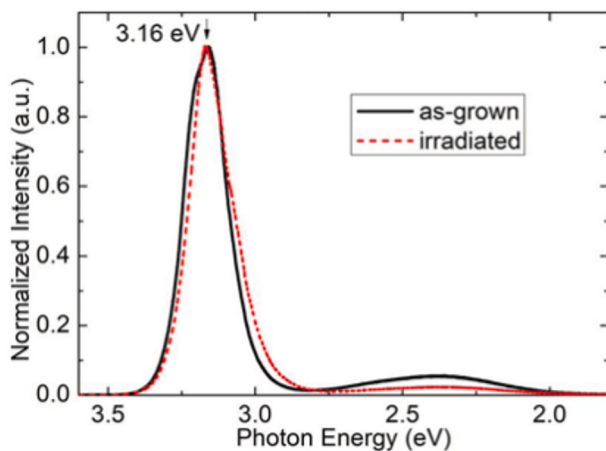


Fig. 8. SEM images of a) as-grown and b) Irradiated ZnO Nanowires (X. Zhao et al., 2019).

irradiated with neutron decreased in diameters while the nanoflakes were transformed into nanoparticle. The shifting of the PL spectra is shown to be slightly apparent for nanoflakes while a slight defect was observed in the nanowire.

Based on a recent study conducted by D. S. et al., 2020 of the effects of neutron flux effect towards the structural properties of a radio frequency sputtered ZnO, it was reported that the structural properties of pre-and post-irradiation of n-ZnO shows that the thin film retains its crystalline properties regardless of exposure towards radiation based on its broad wave. However, observable changes can be noticed on the diffraction peak of the spectra. Unlike gamma-ray, neutron radiation is not able to ionize an atom directly due to their lack of charge. However, neutrons are the only type of radiation that can turn materials radioactive. Once the fabricated samples were prepared, the samples were irradiated at the NUR II facility with a neutron fluence exposure of  $2 \times 10^{14}\text{ n/cm}^2$ ,  $9.5 \times 10^{14}\text{ n/cm}^2$  and  $6.5 \times 10^{15}\text{ n/cm}^2$  utilizing the



**Fig. 9.** Room temperature PL spectra of as grown and irradiated ZnO Nano-wires (X. Zhao et al., 2019).

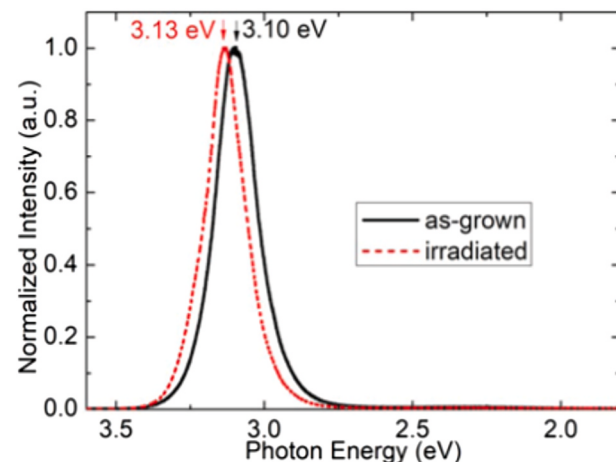


**Fig. 11.** Room temperature PL spectra of as grown and irradiated ZnO nano-flake and nanowire hybrid (X. Zhao et al., 2019).

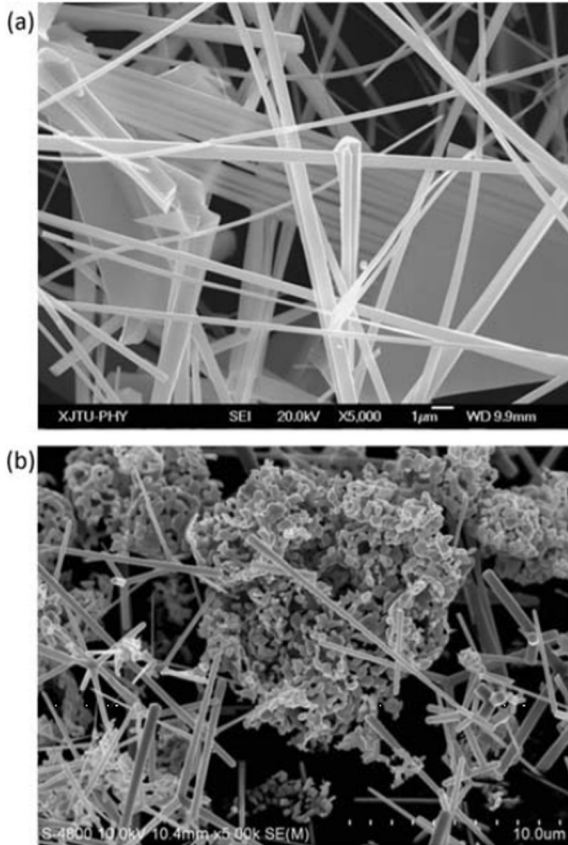


**Fig. 10.** SEM images of a) as-grown and b) Irradiated ZnO Nanoflakes and Nanowire hybrids (X. Zhao et al., 2019).

MINT-TRIGA MARK II reactor.

Based on the reported findings, XRD result shows changes at a flux of  $6.5 \times 10^{15} \text{ n/cm}^2$  may likely be the effect of annealing during exposure. At a maximum flux of  $6.5 \times 10^{15} \text{ n/cm}^2$ , sample shows an FWHM of 0.21 and a crystallite grain size of 32.12 nm based on the XRD analysis. This however might be attributed to the containment chamber with the presence of heat as the damaged induced by neutron is mitigated due to annealing. Fig. 12 shows the XRD spectra.

However, for the electrical properties of ZnO paired CuGaO<sub>2</sub> heterojunction, a drop on the turn-on-voltage is observable at the highest flux of  $6.5 \times 10^{15} \text{ n/cm}^2$ . The increase of the turn-on-voltage may be

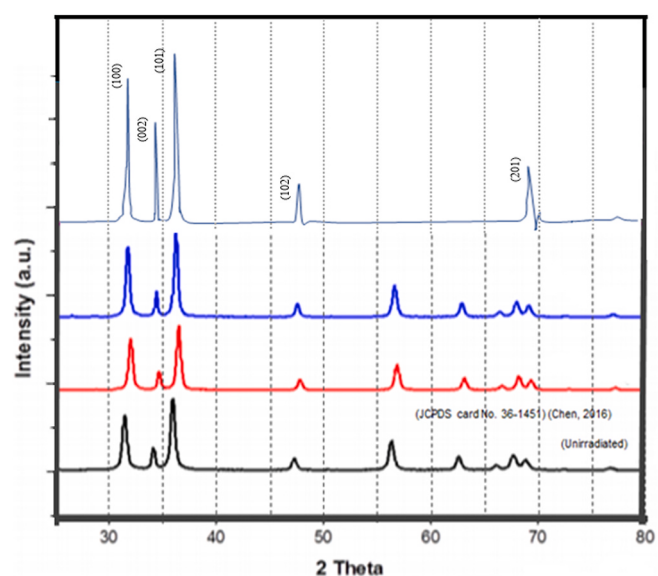


**Fig. 12.** X-ray diffraction (XRD) spectra of ZnO of un-irradiated and irradiated at a flux of  $2 \times 10^{14} \text{ n/cm}^2$ ,  $9.5 \times 10^{14} \text{ n/cm}^2$  and  $6.5 \times 10^{15} \text{ n/cm}^2$  (D. S et al., 2020).

associated with the disruption or distortion of the local lattice structure creating an interstitial-vacancy pair. From the data obtained, neutron flux exposure is only damaging for long period of time exposure. This is because neutron has a short-life and does not last long. The I-V performance of the fabricated heterojunction irradiated under  $2 \times 10^{14} \text{ n/cm}^2$ ,  $9.5 \times 10^{14} \text{ n/cm}^2$  and  $6.5 \times 10^{15} \text{ n/cm}^2$  flux is as shown in Fig. 13.

#### 4.5. Beta damage on ZnO

In general, beta radiation consists of charged particles that are ejected from an atom's nucleus and that are physically identical to electrons. Beta particles generally have a negative charge, are very small and can penetrate more deeply than alpha particles. However, most beta radiation can be stopped by small amounts of shielding, such as sheets of plastic, glass or metal (Claeys and Simoen, 2013). Towards semiconductor, beta radiation will cause direct ionization of the semiconductor atoms resulting in localized heat deposition, and light displacement effects which in turn lead to transient effects of beta irradiation on the semiconductor operating parameters induced due to

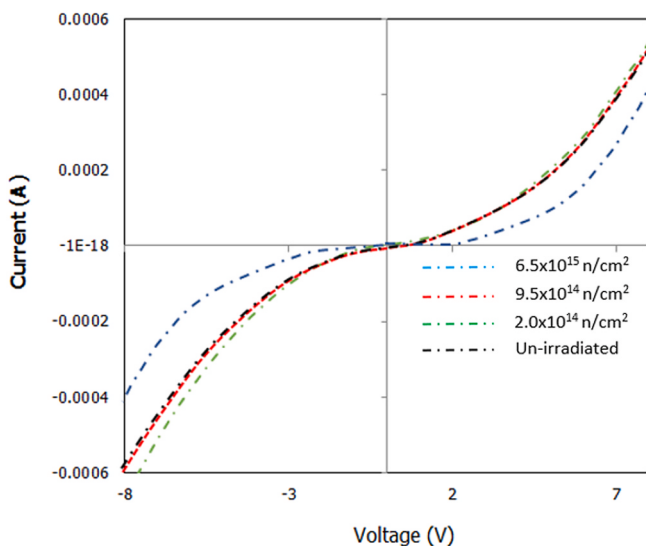


**Fig. 13.** I-V characteristic of n-ZnO/p-CuGaO<sub>2</sub> heterojunction diode at different ionizing dose (D. Zhao et al., 2010).

ionization (Yannakopoulos et al., 2008).

The radiation hardness and optical characteristics of beta- and gamma-irradiated LiNbO<sub>3</sub>(ZnO) crystals had been studied in a wide range of doping levels: ~0.04–5.9 mol% ZnO done by Palatnikov et al. (2018), evaluated as a function of the type and dose of radiation and dopant concentration. The optical damage resistance and radiation hardness of the crystals had been shown to be interrelated and depend on threshold effects in the LiNbO<sub>3</sub>(ZnO). With increasing ZnO concentration, the irradiation colour saturation dose increases: from ~30 Gy in crystal 1, containing ~0.04 mol% ZnO, to ~147 Gy in crystal 6, containing ~5.19 mol% ZnO crystals. This suggests that, increasing the ZnO concentration in the LiNbO<sub>3</sub>(ZnO) crystals reduces the amount of electronic defects capable of recharging and recombining under irradiation. The structural changes responsible for the increase in the optical damage resistance and radiation hardness of the crystals have been shown to be closely interrelated. Moreover, the irradiation effect is strongly dependent on the ZnO concentration both above and below the concentration threshold at ~5.2 mol% ZnO. As a result of structural changes, the optical absorption (transmission) of the “above-threshold” LiNbO<sub>3</sub>(ZnO) crystals remains unchanged even at high irradiation doses.

#### 4.6. Summary: current research work of ionizing radiation on zinc oxide based semiconductor

Table 2 shows the compilation of current research works on Ionizing radiation effects towards ZnO based semiconductor with various types of radiation exposure, dosage and main research findings.

#### 5. Conclusion

This paper presents a review of ZnO tolerance and resistivity towards all kinds of radiation consisted of proton, electron, gamma, neutron and beta. For neutron irradiation, it was shown that at higher flux, the structural properties of the ZnO improves significantly while it does not bode the same for its electrical properties as degradation of electrical parameters were reported with increasing flux attributed to the disruption or distortion of the local lattice structure creating an interstitial-vacancy pair. Despite existing as a secondary product to the primary cosmic radiation and their short life span in space nevertheless, it presents a threat as they can penetrate most man-made construction capable of passing a five feet concrete layer.

Gamma damage has been the most widely studied and understood.

**Table 2**

Author (Year)	Research Focus
Look (2001)	Reviewed on the recent advances in ZnO materials on optical UV lasing, at both low and high temperatures and its resistance towards radiation damage in comparison to common semiconductor materials such as Silicon, Gallium Arsenide, Cadmium Sulfide and even Gallium Nitride irradiated with electron irradiation.
Coskun et al. (2004)	Studied the radiation hardness of ZnO at low temperature, irradiated in a 2 MeV Van de Graaf accelerator at temperatures from 100 to 500 K.
Tuomisto et al. (2005)	Reviewed on the recovery of point defects by irradiating ZnO with electron-irradiation.
Arshak & Korostynska (2006)	Highlighted the response of metal oxide thin film structures by mixing oxides in various proportions and irradiating it with $\gamma$ -rays.
Burlacu et al. (2008)	Studied on the impact of morphology upon the radiation hardness of ZnO layers (Irradiated at room temperature by 130 MeV with Xenon-129 ions at fluences up to $1.5 \times 10^{14} \text{ cm}^{-2}$ ).
Gür et al. (2009)	Highlighted the oxygen effects on the radiation hardness of ZnO thin films by depositing ZnO using electrochemical deposition method with different oxygen flow rates onto an indium tin oxide substrate (ITO) and exposing it to high-energy electron-irradiation (HEEI) (12 MeV). In addition, an annealing process was applied to understand the effect on the recovery of the HEEI-induced defects.
Kristianpoller et al. (2010)	Reviewed on the irradiation effects of beta, X-ray and UV in CaF <sub>2</sub> : ZnO nanostructured crystals.
(D. Zhao et al., 2010)	Reported the effect of gamma ray irradiation with a dose ranging from 10 KGy to 1 MGy towards ZnO thin film transistors and circuits.
Moon et al. (2010)	Studied on the effects of proton irradiation on indium zinc oxide-based thin film transistors with doses up to $10^{12-13} \text{ cm}^{-2}$ .
Lorenz et al. (2011)	Reported on the radiation damage formation and annealing in GaN and ZnO with neutron irradiation a neutron fluence rate of $2.8 \times 10^{13} \text{ n/cm}^2/\text{s}$ ( $E < 0.5 \text{ eV}$ ), a fast fluence rate of $0.6 \times 10^{13} \text{ n/cm}^2/\text{s}$ ( $E > 1 \text{ MeV}$ ), an epithermal fluence rate of $0.1 \times 10^{13} \text{ n/cm}^2/\text{s}$ (at 1 eV) and a gamma dose rate of $2 \times 10^6 \text{ Gy/h}$ .
Indluru et al. (2013)	Focused on the gamma radiation effects on indium zinc oxide thin film transistors.
Ramirez et al. (2013)	Reported on the effects of gamma ray irradiation and electrical stress on ZnO TFTs with a radiation dose of 25 Mrad from a Cobalt-60 source
Al-sofiani et al. (2014)	Studied on the effect of gamma-ray enhanced changes of ZnO:Al thin film structure and optical properties with three different doses of 201.6 KGy, 302.4 KGy and 470 KGy
(Y. Liu et al., 2014)	Focused on the total dose ionizing radiation effects in indium ZnO TFTs using a Cobalt-60 source with a dose rate of 50 rad/s.
Ramirez et al. (2015)	Reported on the application of ZnO thin film transistors for extreme radiation environment with a radiation dose of 240 Krad and 25 Mrad from a Cobalt-60 source
Ramirez et al. (2015)	Reported on the effect of gamma ray exposure for up to 100 Mrad on ZnO TFTs deposited by two different growth techniques: pulsed laser deposition (PLD) and plasma-enhanced atomic layer deposition (PEALD).
Sharma et al. (2017)	Studied on the high performance radiation stable ZnO/Ag/ZnO multilayer transparent conductive electrode, irradiated with 100 MeV Ag <sup>7+</sup> ions of different fluences ranging from $5 \times 10^{11}$ – $5 \times 10^{12} \text{ ions/cm}^2$

Based on this review there is very little research on the structural changes of ZnO properties. In this review discussion on the structural changes due to gamma exposure is reported to have degraded the crystallite grain size, while heat treatment significantly improves the crystallite grain size which restores the electrical conductivity of the irradiated ZnO semiconductor to a nominal operating semiconductor. While on the optical properties, exposure of gamma radiation leads to a decrease in the optical bandgap which is caused by a shift on the transmission edge towards a greater wavelength. The decrease of the

optical bandgap is also attributed to the formation of localized states due to structural defects leading to a decrease in the transition probabilities into the extended states. In regards to refractive index properties, exposure of gamma irradiation causes its value to increase due to the formation of crystal defects. However, there are significant research findings on the electrical properties of ZnO due to gamma irradiation. As a trend, irradiated devices will have an increase in the turn-on-voltage and an increase in oscillation frequency. The increase of the turn-on-voltage is attributed to the increase of ideality factor indicating it is no longer in its ideal state which corresponds to the decrease barrier height. The deterioration of the electrical parameters can also be related to the generation recombination, tunneling interface impurities and interfacial oxide layer defects caused by gamma exposure.

In proton damage, it is seen that the structural properties changes with increasing dose which is apparent in the crystallinity of ZnO thin film is reduced significantly due to either defect isolation or chemical isolation. Observable changes can be seen in post irradiated ZnO where the device has low sensitivities to post thermal annealing treatment due to creation of antisite oxygen point defects which in turn changes the crystallite structure through amorphization. Based on the optical changes it is observed proton irradiation broadens the line width green and a decrease in the photoluminescence intensity. On the electrical properties, a turn-on-voltage shift is observable with increasing proton irradiation dose. The increase in the turn on voltage is caused by the damage induced degradation of carrier mobility in response to the increase of proton fluence.

However, the radiation damage induced by electron shows crystallite structural improvement due to the heating of electron beam changing the amorphous structure of a fabricated ZnO to a crystallite structure. This is further supported by the improvement of the crystallite grain size. On the optical properties, a decrease in the transmittance can be observed due to the loss scattering by the surface crystallites as well as the surface crystallites as well as the surface roughness due to soft cracks in the thin film. Similar to that of proton HEEI also showcase a similar pattern of a PL emission under green emission wavelength.

However, there is still a number of issues where additional work is needed including the reliability of ZnO device due to ionizing radiation and the stability of the devices after irradiation should be understood. In addition, more research should be considered into neutron damage as well as the adverse effects of HEEI on the electrical properties and its similarities to thermal annealing treatment.

### Declaration of competing interest

The authors declare that they have no known competing financial interests or personal relationships that could have appeared to influence the work reported in this paper.

### Acknowledgements

The work is supported by Ministry of Education under the scheme Fundamental Research Grant Scheme FRGS/1/2016/STG02/UMS02/2, Universiti Malaysia Sabah under UMSGreat GUG0387-2/2019 and SDK0075-2019.

### References

- Al-Hamdani, A., Al-Alawy R, N.D., Hassan S, J., 2014. Effect of gamma irradiation on the structural and optical properties of ZnO thin film. Comput. Eng. 16 (1), 11–16. <https://doi.org/10.9790/0661-16191116>.
- Al-sofiani, S.M., Hassan, H.E., Ashour, A.H., El-raheem, M.M.A., 2014. Study of gamma-rays enhanced changes of the ZnO:Al thin Film.pdf. International Journal of Electrochemical Science 9, 3209–3221.
- Amir, H.F.A., Chee, F.P., 2012. Monte Carlo study of alpha ( $\alpha$ ) particles transport in nanoscale gallium arsenide semiconductor materials. AIP Conference Proceedings 1482, 559–563. <https://doi.org/10.1063/1.4757534>.
- Arshak, K., Korostynska, O., 2004. Preliminary studies of properties of oxide thin/thick films for gamma radiation dosimetry. Mater. Sci. Eng. B: Solid-State Materials for Advanced Technology 107 (2), 224–232. <https://doi.org/10.1016/j.mseb.2003.11.014>.
- Arshak, K., Korostynska, O., 2006. Response of metal oxide thin film structures to radiation. Mater. Sci. Eng. B: Solid-State Materials for Advanced Technology 133 (1–3), 1–7. <https://doi.org/10.1016/j.mseb.2006.06.012>.
- Babamoradi, M., Sadeghi, H., Azimirad, R., Safa, S., 2018. Enhancing photoresponsivity of ultraviolet photodetectors based on ZnO/ZnO:Eu ( $x = 0, 0.2, 1, 5$  and  $20$  at.%) core/shell nanorods. Optik 167, 88–94. <https://doi.org/10.1016/j.ijleo.2018.03.127>.
- Bacaksiz, E., Parlak, M., Tomakin, M., Özçelik, A., Karakiz, M., Altunbaş, M., 2008. The effects of zinc nitrate, zinc acetate and zinc chloride precursors on investigation of structural and optical properties of ZnO thin films. J. Alloys Compd. 466 (1–2), 447–450. <https://doi.org/10.1016/j.jallcom.2007.11.061>.
- Badawy, A.A., El-Shafey, S.E., Abd El All, S., El-Shobaky, G.A., 2014. Effect of  $\gamma$ -irradiation and calcination temperature of nanosized ZnO/TiO<sub>2</sub> system on its structural and electrical properties. Adv. Chem. 1–7. <https://doi.org/10.1155/2014/301410>, 2014.
- Burlacu, A., Ursaki, V.V., Skuratov, V.A., Lincot, D., Pauporte, T., Elbelghiti, H., Rusu, E. V., Tiginyanu, I.M., 2008. The impact of morphology upon the radiation hardness of ZnO layers. Nanotechnology 19 (21). <https://doi.org/10.1088/0957-4484/19/21/215714>.
- Chaari, M., Matoussi, A., 2012. Electrical conduction and dielectric studies of ZnO pellets. Phys. B Condens. Matter 407 (17), 3441–3447. <https://doi.org/10.1016/j.physb.2012.04.056>.
- Chee, F.P., Amir, H.F.A., Salleh, S., 2011. Range distribution and electronic stopping power for Cobalt (Co) ions in Gallium Arsenide (GaAs) optoelectronic devices. In: 2011 4th International Conference on Modeling, Simulation and Applied Optimization, ICMSAO 2011. <https://doi.org/10.1109/ICMSAO.2011.5775533>, 0–4.
- Chee, F.P., Duinong, M., Rani, A.I.A., Chang, J.H.W., Alias, A., Salleh, S., 2019. Simulation of displacement damage cross section of cuprous oxide/zinc oxide (Cu<sub>2</sub>O/ZnO) based heterojunction device. J. Eng. Sci. Technol. 14 (4), 1820–1834.
- Cheol Eui, L., Eummo, L., Sucheol, L., W, L., 2010. Radiation damage in proton-irradiated ZnO single crystal. J. Kor. Phys. Soc. 56 (61), 2108. <https://doi.org/10.3938/jkps.56.2108>.
- Claeys, C., Simoen, E., 2002. Radiation Effects in Semiconductor Devices. Springer Berlin Heidelberg.
- Claeys, C., Simoen, E., 2013. Radiation effects in advanced semiconductor materials and devices, (Vol. 57).. Springer Science & Business Media.
- Coskun, C., Look, D.C., Farlow, G.C., Sizelove, J.R., 2004. Radiation hardness of ZnO at low temperatures. Semicond. Sci. Technol. 19 (6), 752–754. <https://doi.org/10.1088/0268-1242/19/6/016>.
- Cressler, J.D., Mantooth, H.A., 2013. Extreme Environment Electronics. CRC Press.
- Mivilid, D.S., Chee, F.P., Rasmidi, R., Alias, A., Salleh, S., Anuar Mohd Salleh, K., Jalal Bayar, A.M., 2020. Gamma ray and neutron radiation effects on the electrical and structural properties of n-ZnO/p-CuGaO<sub>2</sub> Schottky diode. ECS J. Solid State Sci. Technol. 9 (4) <https://doi.org/10.1149/2162-8777/ab8f19>, 045019.
- Di, G., Dong Han, K., Jin, J., 2011. High-performance amorphous indium-gallium-zinc-oxide thin-film transistor with a self-aligned etch stopper patterned by back-side UV exposure. IEEE Electron. Device Lett. 32 (6), 758–760. <http://cat.inist.fr/?aModele=afficheN&cpsidt=24222647>.
- Ellmer, K., Mientus, R., Weiß, V., Rossner, H., 2001. Setup for in situ X-ray diffraction studies of thin film growth by magnetron sputtering. Nucl. Instrum. Methods Phys. Res. Sect. A Accel. Spectrom. Detect. Assoc. Equip. 467–468 (PART II), 1041–1044. [https://doi.org/10.1016/S0168-9002\(01\)00637-4](https://doi.org/10.1016/S0168-9002(01)00637-4).
- Fortunato, E., Barquinha, P., Pimentel, A., Gonçalves, A., Marques, A., Pereira, L., Martins, R., 2005. Recent advances in ZnO transparent thin film transistors. Thin Solid Films 487 (1–2), 205–211. <https://doi.org/10.1016/j.tsf.2005.01.066>.
- Gossick, B.R., 1959. Disordered regions in semiconductors bombarded by fast neutrons. J. Appl. Phys. 30 (8), 1214–1218. <https://doi.org/10.1063/1.1735295>.
- Gupta, K.M., Gupta, N., 2016. Recent Advances in Semiconducting Materials and Devices. Springer International Publishing. <https://doi.org/10.1007/978-3-319-19758-6>.
- Gür, E., Asl, H., Nar, K., Cokun, C., Tüzemen, S., Meral, K., Onganer, Y., Erifoğlu, K., 2009. Oxygen effects on radiation hardness of ZnO thin films. J. Vac. Sci. Technol. B: Microelect. Nanometer Struct. 27 (5), 2232–2237. <https://doi.org/10.1116/1.3222865>.
- Haider, F.A.A., Chee, F.P., 2014. Transient and post-irradiation response of optoelectronic devices to ionizing radiation. J. Phys. Conf. 574 (1) <https://doi.org/10.1088/1742-6596/574/1/012019>.
- Hirao, T., Furuta, M., Furuta, H., Matsuda, T., Hiramatsu, T., Hokari, H., Yoshida, M., Ishii, H., Kakegawa, M., 2007. Novel top-gate zinc oxide thin-film transistors (ZnO TFTs) for AMLCDs. J. Soc. Inf. Disp. 15 (1), 17. <https://doi.org/10.1889/1.2451545>.
- Hui, K.C., Lai, C.W., Ong, H.C., 2005. Electron-beam-induced optical memory effect in metallized ZnO thin films for the application of optical storage. Thin Solid Films 483 (1–2), 222–225. <https://doi.org/10.1016/j.tsf.2004.10.030>.
- Ievskaya, Y., 2014. Fabrication of ZnO/CuO heterojunctions in atmospheric conditions: improved interface quality and solar cell performance. Sol. Energy Mater. Sol. Cell. 135, 43–48. <https://doi.org/10.1016/j.solmat.2014.09.018>.
- Indluru, A., Holbert, K.E., Alford, T.L., 2013. Gamma radiation effects on indium-zinc oxide thin-film transistors. Thin Solid Films 539, 342–344. <https://doi.org/10.1016/j.tsf.2013.04.148>.
- Karuppasamy, A., Subrahmanyam, A., 2007. Effect of electron bombardment on the properties of ZnO thin films. Mater. Lett. 61 (4–5), 1256–1259. <https://doi.org/10.1016/j.matlet.2006.07.014>.

- Kim, J.H., Mirzaei, A., Woo Kim, H., Wu, P., Kim, S.S., 2019. Design of supersensitive and selective ZnO-nanofiber-based sensors for H<sub>2</sub> gas sensing by electron-beam irradiation. *Sensor. Actuator. B Chem.* 293, 210–223. <https://doi.org/10.1016/j.snb.2019.04.113>. April.
- Kinchin, G.H., Pease, R.S., 1955. The displacement of atoms in solids during irradiation. *Solid State Phys.* 2, 307.
- Klochko, N.P., Klepikova, K.S., Petrushenko, S.I., Dukarov, S.V., Kopach, V.R., Khrypunova, I.V., Zhadan, D.O., Lyubov, V.M., Khrypunova, A.L., 2019. Effect of high doses of electron beam irradiation on structure and composition of ZnO films prepared by electrochemical and wet chemical depositions on solid and flexible substrates. *Radiat. Phys. Chem.* 164, 108380. <https://doi.org/10.1016/j.radphyschem.2019.108380>. June.
- Kristianpoller, N., Chen, W., Chen, R., Liu, Y., 2010. Irradiation effects in CaF<sub>2</sub>: ZnO nanostructured crystals. *IOP Conf. Ser. Mater. Sci. Eng.* 15 <https://doi.org/10.1088/1757-899x/15/1/012049>, 012049.
- Lee, E., Lee, S., Lee, W., Lee, C.E., 2010. Radiation damage in a proton-irradiated ZnO single crystal. *J. Kor. Phys. Soc.* 56 (61), 2108–2111. <https://doi.org/10.3938/jkps.56.2108>.
- Lee, K.K., Wang, D., Shinobu, O., Ohshima, T., Kiong, K., Wang, D., Shinobu, O., Ohshima, T., 2018. Reliability of gamma-irradiated n-channel ZnO thin-film transistors: electronic and interface properties. *Radiat. Eff. Defect Solid* 173 (3–4), 250–260. <https://doi.org/10.1080/10420150.2018.1427093>.
- Liu, L.Y., Shen, T.L., Liu, A., Zhang, T., Bai, S., Xu, S.R., Jin, P., Hao, Y., Ouyang, X.P., 2018. Performance degradation and defect characterization of Ni/4H-SiC Schottky diode neutron detector in high fluence rate neutron irradiation. *Diam. Relat. Mater.* 88 (28), 256–261. <https://doi.org/10.1016/j.diamond.2018.07.019>.
- Liu, Y., Wu, W.J., En, Y.F., Wang, L., Lei, Z.F., Wang, X.H., 2014. Total dose ionizing radiation effects in the indium-zinc oxide thin-film transistors. *IEEE Electron. Device Lett.* 35 (3), 369–371. <https://doi.org/10.1109/LED.2014.2301801>.
- Locovei, C., Coman, D., Radu, A., Ion, L., Antohe, V.A., Vasile, N., Dumitru, A., Iftimie, S., Antohe, S., 2019. Physical properties of Cu and Dy co-doped ZnO thin films prepared by radio frequency magnetron sputtering for hybrid organic/inorganic electronic devices. *Thin Solid Films* 685, 379–384. <https://doi.org/10.1016/j.tsf.2019.06.027>. November 2018.
- Look, D.C., 2001. Recent advances in ZnO materials and devices. *Mater. Sci. Eng. B* 80 (1–3), 383–387. [https://doi.org/10.1016/S0921-5107\(00\)00604-8](https://doi.org/10.1016/S0921-5107(00)00604-8).
- Lorenz, K., Peres, M., Franco, N., Marques, J.G., Miranda, S.M.C., Magalhães, S., Monteiro, T., Wesch, W., Alves, E., Wendler, E., 2011. Radiation damage formation and annealing in GaN and ZnO. *Oxide-Based Materials and Devices II* 7940, 794000. <https://doi.org/10.1117/12.879402>. January.
- Luo, C.Q., Ling, F.C.C., Rahman, M.A., Phillips, M., Ton-That, C., Liao, C., Shih, K., Lin, J., Tam, H.W., Djurisic, A.B., Wang, S.P., 2019. Surface polarity control in ZnO films deposited by pulsed laser deposition. *Appl. Surf. Sci.* 483, 1129–1135. <https://doi.org/10.1016/j.apsusc.2019.03.228>.
- Messenger, G.C., Ash, M.S., 1986. The Effects of Radiation on Electronic Systems. Van Nostrand Reinhold Co. <https://doi.org/10.1007/978-94-017-5355-5>.
- Mishra, Y.K., Adelung, R., 2018. ZnO tetrapod materials for functional applications. *Mater. Today* 21 (6), 631–651. <https://doi.org/10.1016/j.mattod.2017.11.003>.
- Moon, Y.K., Lee, S., Moon, D.Y., Kim, W.S., Kang, B.W., Park, J.W., 2010. Effects of proton irradiation on indium zinc oxide-based thin-film transistors. *Surf. Coatings Technol.* 205, S109–S114. <https://doi.org/10.1016/j.surcoat.2010.06.030>. SUPPL. 1.
- Morkoç, H., Özgür, Ü., 2009. Zinc oxide: fundamentals, materials and device technology. In: *Zinc Oxide: Fundamentals, Materials and Device Technology*. <https://doi.org/10.1002/9783527623945>.
- Nastasi, M., Mayer, J.W., Hirvonen, J.K., 1996. *Ion-Solid Interactions: Fundamentals and Applications*. Cambridge University Press.
- Naz, H., Ali, R.N., Liu, Q., Yang, S., Xiang, B., 2018. Niobium doped zinc oxide nanorods as an electron transport layer for high-performance inverted polymer solar cells. *J. Colloid Interface Sci.* 512, 548–554. <https://doi.org/10.1016/j.jcis.2017.10.041>.
- Özgür, Ü., Alivov, Y.I., Liu, C., Teke, A., Reschikov, M.A., Doğan, S., Avrutin, V., Cho, S.J., Morkoç, H., 2005. A comprehensive review of ZnO materials and devices. *J. Appl. Phys.* 98 (4), 1–103. <https://doi.org/10.1063/1.1992666>.
- Palatnikov, M.N., Sidorov, N.V., Makarova, O.V., Panasyuk, S.L., Kurkamkulova, E.R., Yudin, I.V., 2018. Relationship between the optical damage resistance and radiation hardness and the influence of threshold effects on the radiation hardness of ZnO-doped LiNbO<sub>3</sub> crystals. *Inorg. Mater.* 54 (1), 55–59. <https://doi.org/10.1134/S0020168518010120>.
- Parihar, V., Raja, M., Paulose, R., 2018. A brief review of structural, electrical and electrochemical properties of zinc oxide nanoparticles. *Rev. Adv. Mater. Sci.* 53 (2), 119–130.
- Pien, C.F., Abdul Amir, H.F., Salleh, S., Muhammad, A., 2010. Effects of total ionizing dose on bipolar junction transistor. *Am. J. Appl. Sci.* 7 (6), 807–810. <https://doi.org/10.3844/ajassp.2010.807.810>.
- Rahman, M., Al-Ajili, A., Bates, R., Blue, A., Cunningham, W., Doherty, F., Glaser, M., Haddad, L., Horn, M., Melone, J., Mikuz, M., Quinn, T., Roy, P., O’Shea, V., Smith, K., Vaitkus, J., Wright, V., 2004. Super-radiation hard detector technologies: 3-D and widegap detectors. *IEEE Trans. Nucl. Sci.* 51 (5), 2256–2261. <https://doi.org/10.1109/TNS.2004.835902>.
- Ramirez, J.I., Li, Y.V., Basantani, H., Leedy, K., Bayraktaroglu, B., Jessen, G.H., Jackson, T.N., 2015. Radiation-hard ZnO thin film transistors. *IEEE Trans. Nucl. Sci.* 62 (3), 1399–1404. <https://doi.org/10.1109/TNS.2015.2417831>.
- Ramirez, J.I., Li, Y.V., Basantani, H., Jackson, T.N., 2013. Effects of gamma-ray irradiation and electrical stress on ZnO thin film transistors. In: *71st Device Research Conference, DRC 2013 - Conference Digest*, pp. 171–172. <https://doi.org/10.1109/DRC.2013.6633848>.
- Remashan, K., Choi, Y.S., Park, S.J., Jang, J.H., 2012. Impact of near-stoichiometric silicon nitride gate insulator on the performance of MOCVD-grown ZnO thin-film transistors. *ECS J. Solid State Sci. Technol.* 1 (4), 70–78. <https://doi.org/10.1149/2.006204jss>.
- Sahoo, S.K., Mangal, S., Mishra, D.K., Kumar, P., Singh, U.P., 2017. Effect of low energy proton beam irradiation on structural and electrical properties of ZnO:Al thin films. *Mater. Sci. Semicond. Process.* 63, 76–82. <https://doi.org/10.1016/j.mssp.2017.02.002>. January.
- Sahoo, S.K., Mangal, S., Mishra, D.K., Singh, U.P., Kumar, P., 2018. 100 keV H + ion irradiation of as-deposited Al-doped ZnO thin films: an interest in tailoring surface morphology for sensor applications. *Surf. Interface Anal.* 50 (7), 705–712. <https://doi.org/10.1002/sia.6461>.
- Salari, M.A., Güzeldir, B., Sağılam, M., 2018. The effects of gamma irradiation on electrical characteristics of Zn/ZnO/n-Si/Au-Sb structure. *AIP Conference Proceedings* 1935. <https://doi.org/10.1063/1.5025974>.
- Segets, D., Gradi, J., Taylor, R.K., Vassilev, V., 2009. Absorbance spectra for the determination of ZnO nanoparticle size distribution, solubility. *ACS Nano* 3 (7), 1703–1710. <http://www.ncbi.nlm.nih.gov/pubmed/19507865>.
- Sharma, V., Kumar, P., Kumar, A., Surbhi, Asokan, K., Sachdev, K., 2017. High-performance radiation stable ZnO/Ag/ZnO multilayer transparent conductive electrode. *Sol. Energy Mater. Sol. Cell.* 169, 122–131. <https://doi.org/10.1016/j.solmat.2017.05.009>. April.
- Shi, W.S., Agyeman, O., Xu, C.N., 2002. Enhancement of the light emissions from zinc oxide films by controlling the post-treatment ambient. *J. Appl. Phys.* 91 (9), 5640–5644. <https://doi.org/10.1063/1.1466527>.
- Stavale, F., Pascua, L., Nilius, N., Freund, H.J., 2013. Morphology and luminescence of ZnO films grown on a Au(111) support. *J. Phys. Chem. C* 117 (20), 10552–10557. <https://doi.org/10.1021/jp401939x>.
- Tashiro, J., Torita, Y., Nishimura, T., Kuriyama, K., Kushida, K., Xu, Q., Kinomura, A., 2019. Gamma-ray irradiation effect on ZnO bulk single crystal: origin of low resistivity. *Solid State Commun.* 292, 24–26. <https://doi.org/10.1016/j.ssc.2019.01.019>. September 2018.
- Tuomisto, F., Saarinen, K., Look, D.C., Farlow, G.C., 2005. Introduction and recovery of point defects in electron-irradiated ZnO. *Phys. Rev. B Condens. Matter* 72 (8). <https://doi.org/10.1103/PhysRevB.72.085206>.
- Venkatesh, P.S., Jegannathan, K., 2013. Investigations on the growth and characterization of vertically aligned zinc oxide nanowires by radio frequency magnetron sputtering. *J. Solid State Chem.* 200, 84–89. <https://doi.org/10.1016/j.jssc.2013.01.024>.
- Wang, Z.L., 2004. Zinc oxide nanostructures: growth, properties and applications. *J. Phys. Condens. Matter* 16 (25), R829–R858. <https://doi.org/10.1088/0953-8984/16/25/R01>.
- Wesch, W., Wendler, E., Schnohr, C.S., 2012. Damage evolution and amorphization in semiconductors under ion irradiation. *Nucl. Instrum. Methods Phys. Res. Sect. B Beam Interact. Mater. Atoms* 277, 58–69. <https://doi.org/10.1016/j.nimb.2011.12.049>.
- Xie, R., Sekiguchi, T., Ishigaki, T., Ohashi, N., Li, D., Yang, D., Liu, B., Bando, Y., 2006. Enhancement and patterning of ultraviolet emission in ZnO with an electron beam. *Appl. Phys. Lett.* 88 (13), 1–4. <https://doi.org/10.1063/1.2189200>.
- Yannakopoulos, P.H., Skoutzou, A.P., Vesely, M., 2008. Influence of ionizing radiation in electronic and optoelectronic properties of III-V semiconductor compounds. *Microelectron. J.* 39 (5), 732–736. <https://doi.org/10.1016/j.mejo.2007.12.025>.
- You, H.C., Wang, C.J., 2017. Low-temperature, solution-processed, transparent zinc oxide-based thin-film transistors for sensing various solvents. *Materials* 10 (3). <https://doi.org/10.3390/ma10030234>.
- Zhao, D., 2010. Plasma-enhanced Atomic Layer Deposition Zinc Oxide Flexible Thin Film Electronics (Issue December). Pennsylvania State University. <http://adsabs.harvard.edu/abs/2010PhDT.772>.
- Zhao, D., Mourey, D.A., Jackson, T.N., 2010. Gamma-ray irradiation of ZnO thin film transistors and circuits. *Device Research Conference - Conference Digest, DRC 814*, 241–242. <https://doi.org/10.1109/DRC.2010.5551979>.
- Zhao, X., He, Y., Chen, L., 2019. Neutron-irradiation effects on ZnO nanostructure. In: *2019 IEEE International Conference on Electron Devices and Solid-State Circuits, EDSSC 2019*, pp. 1–2. <https://doi.org/10.1109/EDSSC.2019.8754365>.
- Zhou, L., Jackson, T., Brandon, E., West, W., 2004. Flexible substrate a-Si:H TFTs for space applications. *Device Research Conference - Conference Digest, DRC 702*, 123–124. <https://doi.org/10.1109/DRC.2004.1367814>, 1997.